2007

A New N-terminal Recognition Domain in Caveolin-1 Interacts with Sterol Carrier Protein-2 (SCP-2)

Rebecca D. Parr
Stephen F Austin State University, parrrl@sfasu.edu

Gregory G. Martin
Texas A & M University - College Station

Heather A. Hostetler
Texas A & M University - College Station

Megan E. Schroeder
Texas A & M University - College Station

Kiran D. Mir
Texas A & M University - College Station

See next page for additional authors

Authors
Rebecca D. Parr, Gregory G. Martin, Heather A. Hostetler, Megan E. Schroeder, Kiran D. Mir, Ann B. Kier, Judith M. Ball, and Friedhelm Schroeder

A New N-Terminal Recognition Domain in Caveolin-1 Interacts with Sterol Carrier Protein-2 (SCP-2)†

Rebecca D. Parr,‡ Gregory G. Martin,§ Heather A. Hostetler,§ Megan E. Schroeder,‡ Kiran D. Mir,‡,|| Ann B. Kier,‡ Judith M. Ball,*,‡ and Friedhelm Schroeder§

Department of Pathobiology, Texas A&M University, TVMC, College Station, Texas 77843-4467, and Department of Physiology and Pharmacology, Texas A&M University, TVMC, College Station, Texas 77843-4466

Received February 7, 2007; Revised Manuscript Received April 27, 2007

ABSTRACT: Although plasma membrane domains, such as caveolae, provide an organizing principle for signaling pathways and cholesterol homeostasis in the cell, relatively little is known regarding specific mechanisms, whereby intracellular lipid-binding proteins are targeted to caveolae. Therefore, the interaction between caveolin-1 and sterol carrier protein-2 (SCP-2), a protein that binds and transfers both cholesterol and signaling lipids (e.g., phosphatidylinositides and sphingolipids), was examined by yeast two-hybrid, *in vitro* binding and fluorescence resonance energy transfer (FRET) analyses. Results of the *in vivo* and *in vitro* assays identified for the first time the N-terminal amino acids (aa) 1−32 amphipathic α helix of SCP-2 functionally interacted with caveolin-1. This interaction was independent of the classic caveolin-1 scaffolding domain, in which many signaling proteins interact. Instead, SCP-2 bound caveolin-1 through a new domain identified in the N-terminal domain of caveolin-1 between aa 34−40. Modeling studies suggested that electrostatic interactions between the SCP-2 N-terminal aa 1−32 amphipathic α-helical domain (cationic, positively charged face) and the caveolin-1 N-terminal aa 33−59 α helix (anionic, negatively charged face) may significantly contribute to this interaction. These findings provide new insights on how SCP-2 enhances cholesterol retention within the cell as well as regulates the distribution of signaling lipids, such as phosphoinositides and sphingolipids, at plasma membrane caveolae.

Increasing evidence indicates that cholesterol found at the cell-surface plasma membrane (PM) is not randomly distributed but instead organized into both transbilayer (*1*, *2*) and lateral (*3*, *4*) cholesterol-rich (and/or sphingolipid-rich) domains that adopt a unique, liquid-ordered structural organization (*4*−*7*). It has been postulated that this self-assembling property of cholesterol (and also sphingolipids) into domains in turn forms the structural basis for selective membrane protein organization (*8*). Support for this hypothesis is from numerous studies demonstrating that many PM proteins are functionally organized into lipid rafts and/or caveolae, a subfraction of lipid rafts that have proven to be a remarkably stable structural and functional entity (*9*, *10*). Diverse processes, such as transmembrane signal transduction (e.g., eNOS, estrogen, and insulin), the action of microbial (e.g., cholera toxin) and viral (e.g., NSP4) toxins, potocytosis, and microbial (viruses, bacteria, and protozoa) entry into cells, are mediated through PM lipid rafts/caveolae (reviewed in refs *4*, *11*, and *12*). Depletion of cholesterol from the PM lipid rafts/caveolae disrupts these functions. Because of these findings, it has become increasingly important to resolve how cholesterol is transported to lipid rafts/caveolae and how the distribution of cholesterol is regulated within these domains.

Because of the importance of cholesterol to membrane domains and other cell functions, it is not surprising that mammalian cells have evolved multiple pathways for cholesterol entry/efflux. First, unidirectional uptake of cholesteryl ester and cholesterol is mediated by the classic low-density lipoprotein (LDL)[1] receptor/lysosomal endocytic pathway (*13*). Second, unidirectional "selective cholesterol uptake" is mediated by high-density lipoprotein (HDL) binding to scavenger receptor B1 (SRB1) at PM. SRB1 lacks a consensus caveolin "scaffold binding domain" (*14*) and is localized not only in caveolae (e.g., fibroblasts and endothelial cells) but also in lipid rafts of caveolin-1-deficient

† This work was supported in part by the USPHS National Institutes of Health GM31651 (to F.S. and A.B.K.) and GM62326 (to J.M.B.).

* To whom correspondence should be addressed: Department of Pathobiology, Texas A&M University, TVMC, College Station, TX 77843-4467. Telephone: (979) 845-7910. Fax: (979) 845-9231. E-mail: jball@cvm.tamu.edu.

‡ Department of Pathobiology.

§ Department of Physiology and Pharmacology.

|| Current address: Department of Internal Medicine, University of Texas Southwest Medical Center, Dallas, TX 75390.

[1] Abbreviations: aa, amino acids, Cav1, full-length caveolin; caveolin-1−156, C-terminal deletion mutant of caveolin-1 missing most of the C-terminal cytoplasmic domain; Cav 60−178, N-terminal deletion mutant of caveolin-1 missing almost all of the N-terminal cytoplasmic domain except for the signature domain; Cav Δ83−123, caveolin-1 deletion mutant missing part of the caveolin-1 scaffolding domain and part of the transmembrane domain; Cav Δ59−100, caveolin-1 deletion mutant missing all of the scaffolding and signature domains; SCP-2, sterol carrier protein-2; SR-B1, scavenger receptor B1; ABC-A1, ATP-binding cassette protein A1; Pgp, P-glycoprotein; HDL, high-density lipoprotein; LDL, low-density lipoprotein; CSD, caveolin-1 scaffolding domain; CBD, caveolin-1 binding domain; L-FABP, liver fatty acid binding protein; CSM, complete synthetic media; CPRG, chlorophenol red β-D-galactopyranoside assay; 5FOA, 5-fluoroacetic acid; Ura, uracil; PI, phosphoinositol; PtdIns, phosphatidylinositol; PtdIns-4-P, phosphatidylinositol-4-phosphate; PtdIns-4,5-P, phosphatidylinositol-4,5-bisphosphate; M_r, molecular weight.

10.1021/bi7002636 CCC: $37.00
Published on Web 06/20/2007

cells (e.g., hepatocytes) (*14*−*17*). Once bound to SRB1, HDL cholesteryl ester is transferred to the PM lipid rafts/caveolae, internalized by an unresolved, nonendocytic process, and undergoes hydrolysis by nonlysosomal, neutral esterases to free cholesterol (*17*, *18*). Third, unidirectional cholesterol efflux occurs via the ATP-binding cassette transporter A1 (ABCA1) (*19*−*21*), which localizes to lipid rafts/caveolae (*22*, *23*). ABCA1 binds apoprotein-1 (apoA1) to enhance phospholipid efflux, followed by ABCA1-independent cholesterol transfer to the phospholipid containing apoA1, which then becomes HDL (*21*, *24*). Fourth, the bidirectional cholesterol uptake/efflux pathway in which HDL binds to SRB1 is localized in lipid rafts/caveolae rafts and donates/takes up cholesterol by a process that is as yet unclear (*15*, *16*, *21*). Although caveolin-1 expression is associated with increased cholesterol transport to caveolae and increased cholesterol efflux to HDL (*14*, *17*, *25*), SRB1 localization in caveolae is not required for cholesterol uptake/efflux (*15*). While there is considerable evidence that the multidrug resistance transporter P-glycoprotein (P-gp) also participates in SRB1-mediated cholesterol transfer to/from bound HDL, it remains unclear whether P-gp resides in caveolae (*26*), in noncaveolar lipid rafts (*27*), or in an intermediate density membrane microdomain distinct from caveolae and classical lipid rafts (*28*). Many of these proteins appear to indirectly regulate/alter cholesterol flux between the PM and HDL by acting as phospholipid flippases (e.g., ABCA1, P-gp) (*21*, *24*, *28*, *29*). Photo-cross-linking and immunoprecipitation studies show that (i) caveolin-1 (*30*, *31*) but not ABCA1 (*24*) or SRB1 (*14*) directly binds cholesterol, (ii) ABCA1 and SRB1 but not caveolin-1 directly bind HDL (*21*, *22*), (iii) while neither ABCA1, P-gp, or SRB1 contain a caveolin-1 "scaffold binding domain", ABCA1 may interact directly with caveolin-1 (*22*). Thus, when caveolin-1 is directly bound, the ABCA1 may provide a scaffolding platform for cholesterol efflux through either the SRB1 or ABCA1 pathways.

Both vesicular and protein-mediated pathways appear to contribute to intracellular trafficking of cholesterol to and from lipid rafts/caveolae (*4*, *17*, *32*−*34*). At least three cholesterol binding proteins may be involved in protein-mediated cholesterol trafficking through the cytoplasm: caveolin-1, sterol carrier protein-2 (SCP-2), and liver fatty acid binding protein (L-FABP) (*4*, *35*, *36*). Bidirectional flux of free cholesterol and unidirectional uptake of cholesterol ester is thought to be mediated by cytoplasmic transport complexes of caveolin-1, cholesterol (or cholesterol ester), and one or more chaperone proteins (cyclophilin A, cyclophilin 40, heat-shock protein 56, and/or annexin II). The mechanism(s) whereby these complexes dock/interact with PM caveolae appears to involve the CD44 receptor and cytoskeletal proteins (*17*). In contrast to caveolin-1, the other cholesterol binding proteins (L-FABP and SCP-2) have been reported to form simple molecular complexes with cholesterol (but not cholesteryl ester) to (i) enhance cholesterol uptake (SCP-2 $\gg$ L-FABP), (ii) transfer cholesterol between membranes with which they interact (SCP-2 $\gg$ L-FABP), and (iii) transfer cholesterol into bile (L-FABP) (*35*, *37*−*43*). Notably, SCP-2 expression not only enhances cholesterol uptake (*44*) but also stimulates intracellular cholesterol esterification (*45*, *46*) while concomitantly inhibiting cholesterol efflux to HDL (*33*). These findings suggest that caveolin-1 and SCP-2 may have antagonistic effects depending upon the cell context. As of yet, relatively little is known about the mechanism(s) whereby caveolin-1/cholesterol/chaperone, L-FABP cholesterol, and SCP-2 cholesterol complexes dock/interact with PM lipid rafts/caveolae.

Caveolin-1-interacting proteins have been shown to bind the caveolin-1 scaffolding domain (CSD) that resides in amino acids (aa) 80−101 of the central region of caveolin-1 (*47*). The caveolin-1 binding domain (CBD) is comprised of the recognition sequence ΦXΦXXXXΦ or ΦXXXX-ΦXXΦ, where Φ is an aromatic residue (Trp, Phe, or Tyr) (*12*, *48*, *49*). Recent data from our laboratory show SCP-2 is in close proximity to caveolin-1 [i.e., 48 $\pm$ 4 Å, as determined by fluorescence resonance energy transfer (FRET) and immunogold electron microscopy], suggesting a direct interaction with caveolin-1 (*50*). Yeast two-hybrid and co-immunoprecipitation assays confirm these findings (*50*). However, examination of the SCP-2 aa sequence reveals that this protein lacks a consensus caveolin-1 binding domain (*50*). The purpose of the present investigation was to use a series of caveolin-1 mutants and yeast two-hybrid assays to determine (i) if SCP-2 interacts with caveolin-1 through the scaffolding domain and, if not, (ii) whether SCP-2 interacts with another caveolin-1 domain. These studies contribute significantly to our understanding of how SCP-2 participates in intracellular cholesterol trafficking and/or cholesterol uptake/efflux through caveolae.

MATERIALS AND METHODS

Materials. CNBr-activated Sepharose 4B beads were obtained from Amersham Biosciences (Piscataway, NJ). SCP-2 and caveolin-1 peptide-specific antibodies were generated in rabbits in our laboratory as described (*50*−*53*). Rabbit anti-human caveolin-1 was purchased from Jackson Immunoresearch Labs, Inc. (West Grove, CA) or Transduction Labs (San Diego, CA). Bound antibodies were detected by horseradish peroxidase (HRP)-labeled goat anti-rabbit IgG (Kirkegaard and Perry Laboratories, Inc., Gaithersburg, MD or Pierce, Rockford, IL). Total protein was quantitated using the BCA protein assay kit (Pierce). Dulbecco's modified Eagle medium (DMEM) was from Gibco (Grand Island, NY). Fetal bovine serum (FBS), glutamine, penicillin-streptomycin (100 μg/mL), and nonessential amino acid (1X) were from Sigma (St. Louis, MO).

Mammalian Cell Culture. MDCK cells were obtained from ATCC (Rockville, MD) and maintained in DMEM supplemented with 10% FBS, glutamine (2 mM), penicillin-streptomycin (100 μg/mL), and nonessential amino acid (1X). Because of the high expression level of caveolin-1 in MDCK cells (*53*), MDCK lysates were prepared as a source of caveolin-1 antigen. Murine L cells (L arpt-tk-) were cultured as previously described (*54*).

Yeast Strains for Two-Hybrid Assay. Saccharomyces cerevisiae strain MaV203 (MATα, leu2−3,112, trp1−901, his3Δ200, ade2−101, gal4Δ, gal80Δ, SPAL10::*URA3*, GAL1::lacZ, $HIS3_{uas\ gal1}$::*HIS3*@LYS2, $can1^r$, $cyh2^r$) was used for all two-hybrid analyses (*55*). A collection of yeast strains that contain plasmid pairs expressing fusion proteins with a spectrum of interaction strengths [pPC97 (GAL4-DB, LEU2), pPC97-$CYH2^S$, and pPC86 (GAL4-AD, TRP1)] were used as controls (*53*, *56*−*59*). The control plasmids

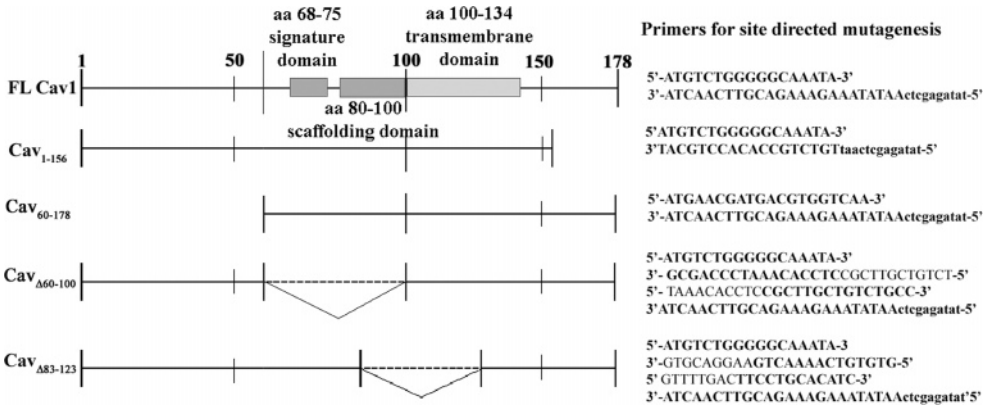

FIGURE 1: Linear schematic of full-length and deletion mutants of caveolin-1. The PCR fragments were produced using the forward and reverse primers listed to the right of each construct and cloned into the DNA-binding domain plasmid, pD22, and the activation-domain plasmid, pD32, of the ProQuest Yeast Two-Hybrid System with Gateway Technology. The full-length clone of caveolin-1 encodes 178 amino acids. One 3′ deletion mutant, Caveolin-1−156, one 5′ deletion mutant, Cav 60−178, and two internal deletion mutants, Cav Δ60−100 and Δ83−123, were produced as described in the Materials and Methods.

pDBleu and pEXP-AD507 contain only the Gal4 DNA-binding domain (BD) and the Gal4 activating domain (AD), respectively.

The *S. cerevisiae* yeast strain InVSc1 (MATα his3-Δ1, leu2, trp1−289, ura3−52; Invitrogen, Carlsbad, CA) was used to induce the production of full-length caveolin-1, mutant caveolin-1, and SCP-2 proteins.

Construction of Plasmids. SCP-2 and full-length caveolin-1 cDNA were cloned into the Invitrogen Gateway Destination vectors pDEST22 and pDEST32 (ProQuest Two-Hybrid System with Gateway Technology Manual, Invitrogen Life Technologies, Inc.) as previously described (*53*, *55*). The deletion mutant clones of caveolin-1, caveolin 1−156, 60−178, Δ60−100, and Δ83−123, were constructed by site-directed mutagenesis using the primers described to the right of the schematic representation of the deletion mutants (Figure 1).

All plasmid manipulations were performed according to standard protocols in the *Escherichia coli* strains DH5α (ProQuest Two-Hybrid System with Gateway Technology Manual, Invitrogen Life Technologies, Inc.). The polymerase chain reaction (PCR) products were directionally cloned into the Gateway System entry vector, pENTR11 (Invitrogen), sequence verified, subcloned into the destination vectors of the Gateway Expression System, pDEST 22 (Gal4 activation domain [AD]-X) and pDEST32 (Gal4 DNA-binding domain [BD]-Y). Briefly, 300 ng of the pENTR11-SCP-2/caveolin-1 plasmids were incubated with 300 ng of the destination vector, pDEST22 or pDEST32, LR buffer, TE (1X), and the LR Clonase Enzyme Mix (Invitrogen). The resultant clones were transformed into DH5α and plated onto LB plates with 100 μg/mL ampicillin or 7 μg/mL gentamycin. After amplification, recombinant plasmids were extracted using the Wizard Miniprep kit (Promega, Madison, WI), restriction-enzyme-digested with *Eco*RV, *Kpn*I, or *Xho*I (Promega), and sequence-verified. Fusion protein expression levels were monitored by Western blot analyses.

Expression of SCP-2, Caveolin-1, and Mutant Caveolin-1 in Yeast. The entry level clones (pENTR11) used to create the yeast two-hybrid expression clones were also employed to introduce the sequences encoding SCP-2, caveolin-1, and mutant caveolin-1 proteins into the inducible yeast expression plasmid, pY52DEST (Invitrogen), as described above. Transformants were first grown on CSMUra$^-$ plates, transferred to liquid CSMUra$^-$, and induced with galactose in YPAG [yeast extract, peptone, and 2% galactose (Difco)] medium to express full-length SCP-2 and caveolin-1 or the four deletion caveolin-1 mutants. Briefly, cells were grown in liquid CSMUra$^-$ medium at 30 °C for 24 h, washed and resuspended at an OD_{600} of 0.5 in YPAG, and incubated at 30 °C for 24 h. Yeast protein cell lysates were prepared using the Zymo Yeast Protein Extraction kit (Zymo Research, Orange, CA) as previously described (*50*) and used in the binding and Western blot assays to detect SCP-2, caveolin-1, or mutant caveolin-1 proteins. Briefly, approximately 1×10^6 cells were pelleted; Y-lysis buffer and zymolase were added; and the samples were incubated at 37 °C for 1 h. The cells were centrifuged at 400 g for 5 min, and supernatants were removed. The pellets were resuspended in phosphate-buffered saline (PBS) with protease inhibitors (100 μM AEBSF, 80 nM Aprotinin, 5 μM Bestatin, 1.5 μM E-64, 2 μM Leupeptin, 1 μM Pepstatin A, and 100 μM PMSF, Calbiochem-Novabiochem Corp., San Diego, CA). The total protein in each pellet was quantitated using the BCA protein assay kit (Pierce). Approximately 10 μg of each pellet was separated on 12% sodium dodecyl sulfate−polyacrylamide gel electrophoresis (SDS−PAGE), transferred to nitrocellulose, and probed with rabbit polyclonal SCP-2 or caveolin-1 antibodies (*50*, *53*). The primary antibodies were detected using goat anti-rabbit-HRP antibodies (Pierce) followed by the addition of the Super Signal Pico West Chemiluminescent Substrate (Pierce), and bands were visualized using X-OMAT film (Kodak).

Yeast Two-Hybrid Screening. S. cerevisiae strain MaV203 (MATα, leu2−3,112, trp1−901, his3Δ200, ade2−101, gal4Δ, gal80Δ, SPAL10::*URA3*, GAL1::lacZ, $HIS3_{uas\ gal1}$::*HIS3*@LYS2, can1^r, cyh2^r) was used to test for protein−protein interactions of SCP-2 and either caveolin-1 or the mutants of caveolin-1 (*58*, *59*). A panel of MaV103 (MATα) control strains containing the same genotype as MaV203 expressing a GAL4 DNA-binding fusion protein (DB−X) and a GAL4 transcription activating protein (AD-Y) with a spectrum of interaction strengths was replica-plated onto assay plates (*49*−*52*). The control vectors were pPC97 (GAL4-DB, LEU2), pPC97-CYH2^S, and pPC86 (GAL4-AD, TRP1). pDBleu and pEXP-AD507 contain only the Gal4

Table 1: Synthetic Peptide Amino Acid Composition and Distribution

peptides	N → C	aa distribution
Cav1 aa 2−31	SGGKYVDSEGHLYTVPIREQGNIYKPNNKA	7C, 7P, 8H
Cav1 aa 19−40	EQGNIYKPNNKAMADELSEKQ	7C, 6P, 4H
Cav1 aa 34−55	DELSEKQVYDAHTKEIDLVNRD	11C, 4P, 6H
Cav1 aa 76−101	EGTHSFDGIWKASFTTFTVTKYWF	4C, 9P, 7H
Cav1 aa 161−178	IEKQLNIRVNSFIKGVAE	4C, 4P, 8H
SCP-2 aa 1−32	SSASDGFKANLVFKEIEKKLEEEGEQFVKKIG	13C, 5P, 8H
SCP-2 aa 1−32E20	SSASDGFKANLVFKEIEKKEEEEGEQFVKKIG	14C, 5P, 7H
Pro-SCP-2 aa 20−0	MGFPEAASSFRTHQIEAVPT	5C, 3P, 12H

DNA-binding domain (BD) and the Gal4 activating domain (AD), respectively. All plasmid manipulations were performed according to standard protocols for the *E. coli* strains DH5α (*48*, *53*, *54*). MaV203 yeast were transformed by a modified lithium acetate (LiAc) procedure as previously described (*56*−*59*). Briefly, *S. cerevisiae* MaV203 were grown in YPAD overnight at 30 °C, diluted to an OD_{600} of 0.5, and incubated at 30 °C with shaking to an OD_{600} of 2. The cells were pelleted, washed with distilled H_2O, resuspended in 1 mL of 100 mM LiAc, pelleted, and resuspended in 0.4 mL of 100 mM LiAc, and 50 μL aliquots were pelleted. The following solutions were added in order: 240 μL of 50% PEG (M_r = 3350), 36 μL of 1 M LiAc, 25 μL of salmon sperm DNA (2 mg/mL), 50 μL of $_dH_2O$, and 100 ng of each plasmid DNA.

Transformants were grown at 30 °C for 3 days on complete synthetic medium lacking leucine and tryptophan ($CSMLeu^-Trp^-$) to identify colonies containing both plasmids. To determine the two-hybrid-dependent transcription activation by SCP-2 and caveolin-1 or mutants of caveolin-1, the induction of the reporter genes, *URA3* and *HIS3*, was evaluated by monitoring the yeast growth patterns on $CSMLeu^-Trp^-Ura^-$, $CSMLeu^-Trp^-$ + 0.2% 5FOA, and $CSMLeu^-Trp^-His^-$ + 3AT (12.5, 50, and 100 mM 3AT) (*50*, *53*). Activation of the *LacZ* promoter was detected qualitatively using the substrate X-gal (5-bromo-4-chloro-3-indolyl-β-D-galactopyranoside). To quantitatively measure β-galactosidase activity, chlorophenol red-β-D-galactopyranoside (CPRG) was used as a substrate (*50*). To ensure that the DB-X or AD-Y fusion proteins do not function as transcription activators, yeast were transformed with the individual fusion constructs and evaluated for growth on all of the media described above.

Western Blot Assays. The colonies that appeared positive for protein−protein interactions as determined by the phenotypic growth patterns were grown in liquid $CSMLeu^-Trp^-$, and yeast protein extracts were prepared using the Zymo Yeast Protein Extraction kit (Zymo Research, Orange, CA). In brief, cells were grown in YPAD medium overnight at 30 °C, and 1×10^6 cells were pelleted, lysed with zymolase, resuspended in PBS at pH 7.2 containing protease inhibitors (above), and quantified by BCA (Pierce). All lysates were separated by 12% SDS−PAGE, electroblotted onto nitrocellulose membranes, and probed with SCP-2 or caveolin-1 peptide-specific antibodies and HRP-conjugated antibodies as previously described (*50*, *53*, *55*).

Protein Purification. The human recombinant mature 13 kDa SCP-2 and 15 kDa pro-SCP-2 were purified as described earlier (*60*). PEX 5C was generously provided by Dr. Jeremy Berg (Johns Hopkins University).

In Vitro Caveolin-1 SCP-2 Binding Assay. To confirm the interactions of caveolin-1 and 13 kDa SCP-2 determined by the yeast two-hybrid assay, an *in vitro* binding assay was developed. Synthetic peptides corresponding to caveolin-1 residues 2−31, 19−40, 34−55, 76−101, and 161−178 (Table 1), a peptide corresponding to mature 13 kDa SCP-2 aa 1−32 (SCP-2_{1-32}), a peptide wherein residue aa20L was mutated to E (SCP-$2_{1-32E20}$), and a peptide corresponding to the 20 aa presequence of pro-SCP-2 (pro-SCP-2_{1-20}) present in 15 kDa pro-SCP-2 (*61*, *62*) were synthesized as described earlier (Table 1) (*63*−*65*). SCP-2 residues 1−32 contain the N-terminal amphipathic α-helical region of mature 13 kDa SCP-2 and represent the membrane interaction domain of SCP-2 (*63*−*65*).

The peptides described above were attached to CNBr-activated Sepharose 4B beads as recommended by the manufacturer (Amersham Biosciences Corp., Piscataway, NJ). Aliquots (2 mg of total protein each) of InVSc-1 (does not express caveolin-1) or MDCK lysate (expresses caveolin-1) were incubated with 50 μL of a 50% slurry Sepharose 4B or Sepharose 4B-SCP-2_{1-32} overnight at 4 °C with gentle mixing. The beads were pelleted by centrifugation, washed 3 times with wash buffer (10 mM Tris at pH 7.5 and 0.5 M NaCl), and resuspended in PBS containing protease inhibitors (above). Half of each sample was separated by 12% SDS−PAGE, transferred to nitrocellulose membranes, and probed with rabbit anti-caveolin-1 in Western blot assays as described above. Interaction(s) of caveolin-1 mutants with SCP-2_{1-32} were monitored also with full-length caveolin-1, caveolin-1−156, and caveolin-160−178 that were expressed in InVSc1 yeast.

To verify the specificity of the reactivity of purified SCP-2 with Cav_{19-40}- and Cav_{34-55}-bound Sepharose beads (Figure 5B), the integrated density value (IDV) for each band was determined using a Fluorochem 8000 Advanced Imager (Alpha Innotech Corp., San Leandro, CA). The average value after background correction was plotted at different concentrations of purified SCP-2 and a constant peptide concentration.

Role of pro-SCP-2 N-Terminal Presequence for Targeting to Peroxisomes: In Vitro FRET. To determine the relative affinity of the C-terminal peroxisomal targeting sequence 1 (PTS-1) present in both SCP-2 and pro-SCP-2, the interaction of these proteins with PEX 5C (peroxisomal receptor for the PTS-1) was examined by FRET. Recombinant PEX 5C was covalently labeled with Cy3 (fluorescence donor), while SCP-2 and pro-SCP-2 were labeled with Cy5 (fluorescence acceptor) by use of a Fluorolink-antibody Cy3 and Cy5-labeling kit (Amersham Biosciences) as indicated by the instructions of the manufacturer. A fixed amount of donor (10 nM PEX 5C) was incubated with increasing amounts of acceptor (Cy5-SCP-2 or Cy5-pro-SCP-2) in PBS at pH 7.4 and 24 °C. Cy3 was excited at 550 nm, and emission was scanned from 560 to 700 nm using a PC1 photon-counting

Table 2: Summary of Phenotypes of Yeast Co-transformed with pD32-Caveolin-1 Mutants and pD22-SCP-2

		CSM-Leu-Trp-His + 3AT[a]						
	CSM-Leu-Trp[b]	12.5 mM	50 mM	100 mM	CSM-Leu-Trp-Ura[c]	CSM-Leu-Trp + 0.2% 5FOA[d]	**β-gal CPRG**[e]	phenotype[f]
2+ positive	+	±	−	−	−	−	+ 5.890	positive
1+ positive	+	+	+	±	±	±	± **0.202**	positive
negative	+	+	±	±	−	+	− 0.072	negative
caveolin-1	+	+	−	−	−	±	± **1.755**	positive
Cav 1−156	+	+	−	−	−	±	+ 1.050	positive
Cav 60−178	+	+	±	−	−	+	− 0.068	negative
Cav Δ83−123	+	+	−	−	−	±	+ 1.243	positive
Cav Δ60−100	+	−	−	−	−	±	+ 0.390	positive

[a] Colonies were replica-plated onto complete synthetic medium lacking Leu, Trp, and histidine (−His) with 12.5, 50, or 100 mM 3-amino-triazole. [b] Colonies were streaked onto complete synthetic medium lacking leucine (−Leu) and tryptophan (−Trp). [c] Colonies were replica-plated onto complete synthetic medium lacking Leu, Trp, and uracil (−Ura). [d] Colonies were replica-plated onto complete synthetic medium lacking Leu and Trp with 0.2% 5-fluorooratic acid (5FOA). [e] Colonies were replica-plated onto yeast peptone A dextrose plates with nitrocellulose filters. A qualitative β-galactosidase assay was performed using X-gal, resulting in +, ±, or −. A qualitative CPRG assay was performed and reported as β-galactosidase units. [f] Phenotype was determined by combining the results from the differential media to determine a protein−protein interaction.

spectrofluorometer (ISS, Inc., Champaign, IL). The data were corrected for background (buffer only, donor only, and acceptor only). Binding affinities were calculated from the quenching of Cy3 fluorescence intensity ($F_o - F$) at 570 nm with an increasing acceptor concentration as described earlier (*66*). The intermolecular distance was calculated as shown previously using the known critical distance for 50% efficiency (i.e., 50 Å) for the Cy3/Cy5 FRET pair (*67*).

Laser Scanning Confocal Microscopy (LSCM) of SCP-2 Colocalization with Caveolae/Lipid Raft Marker GM₁ at the PM of Living Cells. Murine L cells (L arpt-tk-) were seeded onto Lab-Tek chambered cover glass slides as previously described (*54*). Culture medium was replaced with 0.5 mL of serum-free media containing 0.7 μg of protein (Cy5-labeled SCP-2 or Cy5-labeled pro-SCP-2 prepared as described above) per chamber well and incubated at 37 °C and 5% CO_2 in a humidified chamber for 1 h. Thereafter, 1 mL of complete media (containing serum) was added to each chamber well, and cells were incubated for an additional 2 h as described above. Cells were washed with 1 mL of cold PBS 4 times and, after the final wash, incubated at 4 °C for 10 min. PBS wash was replaced with cold PBS containing 0.4 μg/mL cholera toxin B-AF488 (Invitrogen Corp.), and cells were incubated at 4 °C for an additional 5 min before imaging. Cholera toxin B is a select marker for ganglioside M_1 (GM_1) in caveolae/lipid rafts (*7*, *51*). LSCM was performed with a MRC-1024 fluorescence imaging system (Bio-Rad, Hercules, CA) equipped with an Axiovert 135 microscope and X63 Plan-Fluor oil immersion objective, N.A.1.45 (Zeiss, Carl Zeiss, Inc., Thornwood, NY). AlexaFluor 488 and Cy5 probes were excited at 488/647 lines with a krypton−argon laser (5 mW, all lines) (Coherent, Sunnyvale, CA) set at 10% scan strength, and emission was simultaneously recorded by separate photomultipliers after passing through a 540/30 or 680/32 emission filter, respectively, under manual gain and black level control.

RESULTS

SCP-2 Interacts with Caveolin-1 in a Yeast Two-Hybrid Assay. Although SCP-2 lacks a CBD consensus sequence for interacting with the CSD, the possibility was considered that SCP-2 may still interact through some other interaction with this domain or with another region of caveolin-1. The sequences encoding SCP-2, full-length caveolin-1 (caveolin-1 1−178), and caveolin-1 deletion mutants (Figure 1) were cloned into the ProQuest (Invitrogen) vectors pDEST32 and pDEST22 to produce fusion proteins encoding the GAL4 DNA-binding domain and activating domain, respectively. The resultant plasmids were co-transformed into yeast (MaV203) and initially grown on CSMLeu$^-$Trp$^-$ plates with transformation efficiencies of ∼2−5 × 10^6 transformants/μg of plasmid DNA (data not shown). These data are in the range of the standard efficiencies of greater than 1 × 10^6 transformants/μg of plasmid DNA (*49*).

Co-transformed yeast were monitored for growth on media lacking specific aa and incorporating specific growth inhibitors. Four phenotypes, His$^+$(3AT^R), β-gal, Ura$^+$, and 5FOA^S, were used to assess the activation of the chromosomally integrated reporter genes, *HIS3*, *URA3*, and *LacZ*. The control yeast that are supplied with the ProQuest Two-Hybrid System and the transformants grew on plates with CSMLeu$^-$Trp$^-$, demonstrating the presence of both co-transformed plasmids, pDest32 and pDest22 vectors (Table 2). Induction of the *URA3* gene was shown with growth on CSMLeu$^-$Trp$^-$Ura$^-$ plates and the inhibition of growth on CSMLeu$^-$Trp$^-$ + 0.2% 5FOA. The *URA3* promoter, SPO13, previously has been shown to be a weak promoter, yielding a low growth of yeast on plates lacking uracil. The data presented in Table 2 were consistent with this finding. Induction of *HIS3* was demonstrated by showing an increased 3AT dose-dependent level of inhibition of growth on CSMLeu$^-$Trp$^-$His$^-$ + 3AT in agreement with the *URA3* data (Table 2). The induction of *LacZ* resulted in positive yeast colonies turning a blue color when assayed on nitrocellulose membranes using X-gal as the substrate (data not shown). All colonies that demonstrated phenotypes interpreted by the four reporter gene readouts as "possible interactors" with weak to little production of β-galactosidase and/or uracil were confirmed and quantitated using the liquid CPRG assay for *LacZ* expression (Table 2). When the data are taken together, the growth patterns of the co-transformed yeast confirmed the activation of the three reporter genes in the yeast two-hybrid assays and established SCP-2 and caveolin-1 as forming a true protein−protein interaction.

Localization of the Binding Site of SCP-2 to the N-Terminal Region of Caveolin-1. The following deletion mutants were utilized to determine the region of caveolin-1 that interacts with SCP-2: (i) Caveolin-1 1−156, a C-terminal deletion mutant of Cav-1 missing most of the C-terminal cytoplasmic domain, (ii) Cav 60−178, an N-terminal deletion mutant of caveolin-1 missing almost all of the N-terminal cytoplasmic domain except for the signature

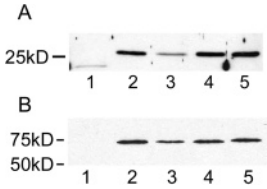

FIGURE 2: Expression of SCP-2- and caveolin-1-fusion proteins in co-transformed yeast. Untransfected (lanes 1) and co-transfected MaV203 yeast cell lysates containing pD32Cav1Δ83−123 (lanes 2), pD32Cav1Δ60−100 (lanes 3), pD32Cav1 1−156 (lanes 4), and pD32Cav1 (lanes 5) were separated on 12% SDS−PAGE and transferred onto nitrocellulose membranes. The blots were probed with rabbit anti-SCP-2_{1-32} (A) or anti-Cav_{2-31} (B) followed by goat anti-rabbit HRP-conjugated secondary antibodies.

domain, (iii) Cav Δ83−123, a caveolin-1 deletion mutant missing part of the caveolin-1 scaffolding domain and part of the transmembrane domain, and (iv) Cav Δ60−100, a caveolin-1 deletion mutant missing all of the scaffolding and signature domains. Yeast co-transformed with pD22-caveolin-1, -caveolin-1 1−156, -Cav Δ83−123, -Cav Δ60-100, and pD32-SCP-2 demonstrated the correct phenotypes (interaction with SCP-2) on the selection media and β-galactosidase activity equal to or greater than the 1+ positive control (data not shown). Likewise, when caveolin-1 and mutants were cloned into pD32 and co-transformed with pD22-SCP-2, the correct phenotypes (interaction with SCP-2) on the selection media were observed and β-galactosidase activity was equal to or greater than the 1+ positive control (Table 2). However, yeast co-transformed with the fusion construct, pD32Cav 60−178, and pD22-SCP-2 failed to demonstrate the correct phenotypes on the test media for a protein−protein interaction and were negative for β-galactosidase activity in both the X-gal assay (data not shown) and CPRG assay (Table 2). These results strongly suggest that caveolin-1 does not bind SCP-2 through the scaffolding domain, the C-terminal cytoplasmic tail, or the signature domain. Instead, the binding site of caveolin-1 for SCP-2 was localized to the N-terminal cytoplasmic domain comprised of caveolin-1 residues 1−59.

SCP-2 and Caveolin-1-GAL4 DNA-Binding Domain- and Activating Domain-Fusion Proteins Were Present in the Co-transformed Yeast. Expression of both fusion proteins in cotransformed yeast was confirmed by Western blot analyses (Figure 2). The GAL4 fusion proteins were observed when the yeast lysates were electroblotted and probed with either SCP-2-specific peptide antibodies or caveolin-1 antibodies (Figure 2). In Figure 2A, the co-transformed yeast lysates containing pD32-caveolin-1 full length or mutants and pD22-SCP-2 showed a SCP-2 fusion protein at the same M_r (~25.5 kD, lanes 2−5). Whereas in Figure 2B, the caveolin-1 fusion proteins were seen as a dimer (M_r between 60 and 78 kD). For example, pD32-cav Δ83−123 should run at ~62.8 kD because Gal4 calculates as ~16.8 kD and cav Δ83−123 as ~14.6 kD, making the monomer ~31.4 kD and the dimer ~62.8 kD (lane 2), and pD32-caveolin-1 calculates to ~38.8 kD monomer and ~77.6 kD dimer (lane 5). These data corroborated that the fusion proteins encoded on both plasmids were translated in the yeast.

Direct Interaction of Caveolin-1 with SCP-2 in Vitro: Role of the SCP-2 N Terminus. The caveolin-1 scaffolding domain (aa 80−100) represents not only the binding sites for numerous proteins (*48*, *49*) but also the membrane lipid raft binding site (*68*, *69*). By analogy, although the SCP-2 N-terminal aa 1−32, an amphipathic α-helix structure (i.e.,

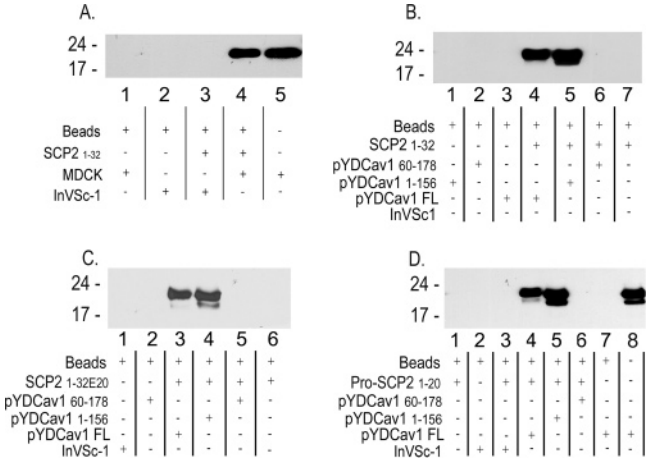

FIGURE 3: SCP-2_{1-32} binding assays: MDCK cell lysates and yeast expressing caveolin-1 (pY52DCav1). MDCK or InVSc-1 cell lysates were incubated with the immobilized SCP-2_{1-32} (Sepharose-4B-SCP-2_{1-32}), separated on 12% SDS−PAGE, transferred to nitrocellulose membranes, probed with rabbit caveolin-1 antisera, and detected as described in the Materials and Methods. (A) Analysis of MDCK (lane 4) and InVsc-1 (lane 3) lysates reacted with Sepharose-4B-SCP-2_{1-32}. Beads only with each of the lysates served as a negative control (lanes 1 and 2). Unreacted MDCK lysates was utilized as the positive control (lane 5). (B) Sepharose-4B-SCP-2_{1-32} reacted with yeast lysates expressing full-length caveolin-1 (lane 4) and caveolin-1 deletion mutants, Cav1 1−156 (lane 5) and Cav1 60−178 (lane 6). Each lysate was reacted with beads only (lanes 1−3) to show specificity with SCP-2_{1-32}. Lane 7 shows beads and peptide only. (C) Sepharose-4B-SCP-$2_{1-32E20}$ reacted with yeast lysates expressing full-length caveolin-1 (lane 3) and caveolin-1 deletion mutants, Cav1 1−156 (lane 4) and Cav1 60−178 (lane 5). Beads with no peptide were reacted with lysates from either untransformed yeast (InvSC-1) or yeast expressing Cav1 60−178 (lanes 1 and 2, respectively) to show specificity with SCP-$2_{1-32E20}$. Lane 6 shows beads and peptide only. (D) Sepharose-4B-pro-SCP-2_{1-20} reacted with yeast lysates expressing full-length caveolin-1 (lane 4) and caveolin-1 deletion mutants, Cav1 1−156 (lane 5) and Cav1 60−178 (lane 6). Lysates were reacted with beads only (lanes 2 and 7) to show specificity with SCP-2_{1-32}. Lane 1 shows beads and peptide only. Lane 8 shows the specificity of the antibody for caveolin-1 expressed from full-length caveolin-1.

hydrophobic and cationic faces), comprises an SCP-2 structural domain for the interaction with model membranes containing anionic phospholipids (*63*−*65*), it is not known whether SCP-2_{1-32} comprises a protein binding (e.g., caveolin-1) domain. To begin to resolve this issue, the N-terminal SCP-2_{1-32} was synthesized, coupled to Sepharose 4B beads, and used in an *in vitro* binding assay, wherein caveolin-1 binding was detected by Western blot analyses. Synthetic peptides corresponding to caveolin-1 residues 2−31, 19−40, 34−55, 76−101, and 161−178 (Table 1), a peptide corresponding to mature 13 kDa SCP-2 aa 1−32 (SCP-2_{1-32}), a peptide wherein residue aa20L was mutated to E (SCP-$2_{1-32E20}$), and a peptide corresponding to the 20 aa presequence of pro-SCP-2 (pro-SCP-2_{1-20}) present in 15 kDa pro-SCP-2 (*61*, *62*) were synthesized as described earlier (Table 1) (*63*−*65*). To confirm the *in vivo* yeast two-hybrid assay that identified the caveolin-1 N domain as the interaction site with SCP-2, the *in vitro* peptide binding assay was repeated using yeast lysates expressing full-length caveolin-1 (pY52DCaveolin-1), a caveolin-1 mutant with the putative binding site present (e.g., pY52DCaveolin-1 1−156), and an N-terminal deletion mutant of caveolin-1 with the putative binding site deleted (e.g., pY52DCav 60−178) (Figure 3B). The lack of reactive bands in lanes 1, 2, 3, and 7 (Figure 3B) showed the lack of nonspecific binding of the

Sepharose-4B beads and specificity of the antibody. SCP-2_{1-32}-linked beads bound to full-length α-caveolin-1 but not *β*-caveolin-1 (lane 4 in Figure 3B). In contrast, SCP-2_{1-32}-linked beads bound to both α- and *β*-caveolin-1 1−156, missing the C terminus (lane 5 in Figure 3B). Cav 60−178 failed to bind the SCP-2_{1-32}-linked beads (lane 6). When these findings are taken together, they not only confirm that the SCP-2_{1-32} binding site is localized to the N terminus of α-caveolin-1 but also that the interaction with the shorter *β*-caveolin-1 (missing the N-terminal 32 aa present only in α-caveolin-1) became more prominent upon deletion of the caveolin-1 C terminus. These data suggest that the N-terminal SCP-2 interacted with the N terminus of full-length α-caveolin-1 but interacted with *β*-caveolin-1 only when the α-caveolin-1 C terminus was missing.

Because SCP-2_{1-32} bound the N terminus of caveolin-1, it was important to determine if this correlated with the ability of this SCP-2 domain to bind anionic phospholipids. SCP-2_{1-32} contains an amphipathic helical region containing a basic face, which directly interacts with anionic phospholipids in model membranes (*63*, *64*). Therefore, the amphipathic helical region of SCP-2_{1-32} was disrupted by replacing Leu20 with Glu20 to produce the mutant peptide SCP-$2_{1-32E20}$. In this study, SCP-$2_{1-32E20}$ was coupled to beads and binding to caveolin-1 was determined with the *in vitro* peptide binding assay using yeast lysates expressing full-length caveolin-1 and caveolin-1 deletion mutants. SCP-$2_{1-32E20}$ interacted with full-length α-caveolin-1 (lane 3 in Figure 3C) and with caveolin-1 deletion mutants, Caveolin-1 1−156 (lane 4 in Figure 3C), but not with the Cav 60−178 (lane 5 in Figure 3C). Again, Western blotting also showed that SCP-$2_{1-32E20}$ primarily interacted only with the full-length α-caveolin-1 form (lane 4 in Figure 3C), but also interacted with the *β*-caveolin-1 when the C terminus was deleted (lane 4 in Figure 3C). Note that SCP-$2_{1-32E20}$ does not bind to anionic phospholipids (*63*, *64*) and does not exhibit lipid-transfer activity (*70*). Thus, the ability of SCP-2_{1-32} to interact with the N-terminal region of caveolin-1 shown herein is independent of its ability to bind to anionic phospholipids (*63*, *64*) and elicit lipid transfer (*70*).

To determine if the 20 aa presequence present in pro-SCP-2 also interacted with caveolin-1, pro-SCP-2_{1-20} was linked to beads and tested for binding to full-length and mutant caveolin-1. Pro-SCP-2_{1-20}-linked beads predominantly bound to full-length α-caveolin-1 (lane 4 in Figure 3D), whereas Pro-SCP-2_{1-20} bound to both α- and *β*-caveolin-1 when the caveolin-1 C terminus was deleted (lane 5 in Figure 3D) but not to Cav 60−178 (lane 6 in Figure 3D). Lane 8 of Figure 3D shows that the yeast express both isoforms of caveolin-1. Thus, in the mature SCP-2, the caveolin-1 binding site was localized in SCP-2_{1-32}, while in the pro-SCP-2 precursor, the 20 aa N-terminal presequence also bound. When these data are taken together, they indicate that the SCP-2 caveolin-1 binding site is localized to the N terminus, as suggested with the yeast two-hybrid data, and the caveolin-1 binding also occurs with the 20 aa presequence present in pro-SCP-2.

To examine the caveolin-1−SCP-2 interaction in greater detail, synthetic peptides corresponding to caveolin-1 residues 2−31, 19−40, 34−55, 76−101, and 161−178 were synthesized and attached to CNBr-activated Sepharose 4B beads. In addition, SCP-2 was purified to test the reactivity to the different caveolin-1 peptides in a direct binding assay. The silver stain (inset) and mass chromatogram show the purity of the SCP-2 protein (Figure 4).

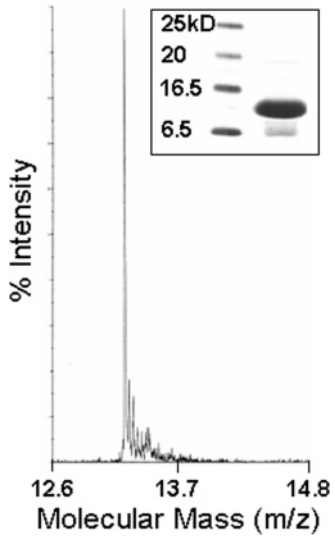

FIGURE 4: Mass spectrum and SDS−PAGE analysis of purified recombinant SCP-2. SCP-2 was IPTG-induced and purified from the *E. coli* strain, W3110, and examined by mass spectrometry and SDS−PAGE with silver stain. The matrix-assisted laser desorption ionization time-of-flight (MALDI−TOF) mass spectrum of SCP-2 is shown. The inset is a photograph of a silver-stained gel after SDS−PAGE of molecular-size markers (lane 1) and 10 mg of SCP-2 (lane 2).

Purified SCP-2 and recombinant yeast lysates expressing SCP-2 were reacted with the panel of caveolin-1 synthetic peptides bound to Sepharose beads (Figure 5). Note in all assays the beads alone (no peptide) incubated with InVSc1 lysates were nonreactive. In Figure 5A, Cav_{2-31}-bound beads also failed to react with InVSc1 or pY52D-SCP-2 (lanes 2 and 5, respectively). Similarly, Cav 76−101 and 161−178 failed to bind purified SCP-2 (data not shown) or SCP-2 expressed in yeast (parts C and D of Figure 5). When the caveolin-1 N-terminal peptides, $Cav1_{19-40}$ and $Cav1_{34-55}$, were reacted with purified SCP-2, a strong interaction was noted (lanes 2 and 3 in Figure 5B). However, there was a minor interaction between the beads alone with purified SCP-2 (lane 1 in Figure 5B). This pattern was repeatedly observed with purified SCP-2 varying in concentration from 50 to 200 ng and a constant concentration of bound-peptide or beads alone. To rectify this background reactivity, the IDV of equal areas was established for each concentration of SCP-2 reacted against the N-terminal caveolin-1 peptides. The IDV of the light band corresponding to beads alone and SCP-2 were subtracted from the positive values and plotted (Figure 5E). As shown with both 200 and 50 ng of purified SCP-2, the IDV of SCP-2 and Cav_{19-40} was consistently higher than that observed with Cav_{34-55}, suggesting that SCP-2 had a higher affinity for Cav_{19-40} than for Cav_{34-55} (Figure 5E). When these data are taken together, they indicate a specific interaction between SCP-2 and Cav_{19-40} and Cav_{34-55}, with a stronger binding with Cav_{19-40}.

In summary, the results of the *in vivo* yeast two-hybrid assays indicated that the caveolin-1 cytoplasmic N-terminal 59 aa contained the SCP-2 binding domain. The *in vitro* binding assays using SCP-2_{1-32} confirmed that the N terminus of SCP-2 binds to an N-terminal region of caveolin-1 and refined the SCP-2 binding site to the first 32

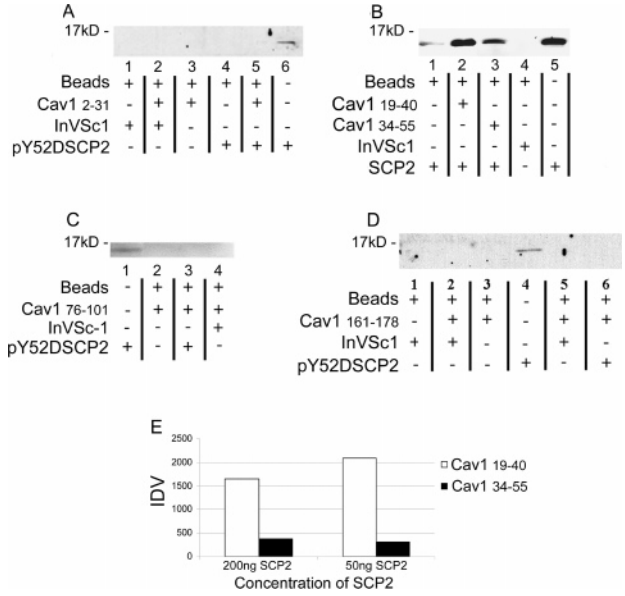

FIGURE 5: Absence of SCP-2 binding to mutant caveolin-1 peptides (Cav1 2−32 and Cav1 167−178) coupled to Sepharose beads. Caveolin-1 synthetic peptides (aa 2−31, 19−40, 34−55, 76−101, and 161−178) were linked to Sepharose beads and reacted with InVSc-1 only (negative control), yeast expressing SCP-2 (A, C, and D) or purified recombinant SCP-2 (B). Peptides bound to beads were reacted with SCP-2, washed, separated on a 12% SDS−PAGE, transferred to nitrocellulose, and reacted with anti-sera specific to SCP-2. (A) Yeast expressing SCP-2 only (lane 6) or reacted with beads only (lane 4) or beads bound by the N-terminal caveolin-1 peptide (aa 2−31, lane 5). (B) Purified recombinant SCP-2 (lane 5) was reacted with Sepharose beads bound with $Cav1_{19-40}$ (lane 2) or $Cav1_{34-55}$ (lane 3). InVSc1 and beads only are shown in lane 4, and purified SCP-2 with unbound beads is shown in lane 1. (C and D) Akin to A, yeast expressing SCP-2 were reacted with caveolin-1 peptide-bound Sepharose beads. C shows reactivity with the $Cav1_{76-101}$ (lane 3), and D shows reactivity with $Cav1_{161-178}$ (lane 6). Controls in both panels included InVSc1 (C, lane 4; D, lanes 2 and 5), expressed SCP-2 only (C, lane 1; D, lane 4), and beads only (no peptide) (D, lane 1). (E) Because of the low reactivity with purified SCP-2 and beads only (see B, lane 1), additional studies were performed using different concentrations of SCP-2 and constant concentrations of Sepharose beads only or bound to peptides. These results are graphically shown in E. The *y* axis shows the average IDV equivalent to IDV/area. The *x* axis shows the concentration of purified recombinant SCP-2 reacted with $Cav1_{19-40}$ (□) or $Cav1_{34-55}$ (■). The values of the average IDV acquired with SCP-2 reacted with beads only were subtracted from the average IDV of SCP-2 reacted with peptide-bound beads and therefore not shown.

residues (Figure 7). Subsequent caveolin-1 peptide binding assays using purified or recombinant SCP-2 localized the binding domain of SCP-2 to caveolin-1 to $Cav1_{19-40}$ and $Cav1_{34-55}$ or caveolin-1 residues 19−55, which can be further defined to aa 32−55 when considering the negative binding results of SCP-2 to $Cav1_{2-31}$. (Figures 5 and 7). These data further indicated a stronger reactivity between SCP-2 and the 19−40 caveolin-1 peptide when compared to the 34−55 peptide.

Role of the N-Terminal Presequence of pro-SCP-2 in Receptor Interactions in Vitro. As indicated above, the 20 aa presequence of pro-SCP-2 also interacted with caveolin-1, albeit the functional significance of this finding is not known. Western blot analyses detect only the mature SCP-2, suggesting that the pro-SCP-2 interaction is not physiologically significant (reviewed in ref *39*). However, convincing evidence has been presented that demonstrates that the pro-SCP-2 is significantly more targeted to peroxisomes, where the 20 aa presequence is proteolytically cleaved (reviewed in ref *39*). This suggests that the 20 aa presequence might be more important for the interaction of the pro-SCP-2 with the peroxisomal receptor (PEX 5C), in which the peroxisomal targeting sequence 1 is present in the C terminus of pro-SCP-2 as well as SCP-2. To examine the latter possibility, a FRET assay was used to determine binding affinities of PEX5C for pro-SCP-2 versus SCP-2 as described in the Materials and Methods. PEX5C bound pro-SCP-2 with high affinity, K_d of 2.3 nM, over 12-fold stronger than that for SCP-2 (Table 3). Consistent with the close molecular interaction between PEX5C and these proteins, the respective intermolecular distances were both near 70 Å (Table 3). Further, the intermolecular distance between pro-SCP-2 and PEX5C in the complex was slightly larger than between SCP-2 and PEX5C, reflecting the larger size of the 15 kDa pro-SCP-2 as compared to 13 kDa SCP-2 (Table 3). These data indicate that the pro-SCP-2 interacts significantly more strongly with the peroxisomal receptor PEX5C than does SCP-2 ($p < 0.05$).

Role of the N-Terminal Presequence of pro-SCP-2 in Determining SCP-2 Distribution to PM Lipid Rafts in Living Cells. To determine if the presence of the N-terminal presequence in pro-SCP-2 resulted in less targeting to PM caveolae/lipid rafts, SCP-2 was colocalized with GM_1 (caveolae/lipid raft marker) by LSCM. When L cells were incubated with the same amounts of Cy5-SCP-2 or Cy5-pro-SCP-2 as described in the Materials and Methods, these proteins were taken up by the cells to a similar extent (not shown). However, labeling of the intact cells with cholera toxin B-AF488 (marker for GM_1) revealed significant differences in colocalization at PM caveolae. When Cy5 and cholera toxin B-AF488 were simultaneously imaged through separate photomultipliers by LSCM, regardless of whether Cy5- SCP-2 (Figure 8A) or Cy5-pro-SCP-2 (Figure 8C) were incorporated into the cells, cholera toxin B-AF488 labeled GM_1 primarily at the cell surface. Some punctuate cholera toxin B-AF488 fluorescence appeared below the PM, reflecting the known very rapid endocytic uptake of L cells (*71*, *72*). A representative image of cells incubated with Cy5-SCP-2 and cholera toxin B-AF488 showed that some Cy5-SCP-2 colocalized with cholera toxin B-AF488 labeled GM_1 at the PM (Figure 8B). In contrast, there was much less colocalization in cells incubated with Cy5-pro-SCP-2 and cholera toxin B-AF488 (Figure 8D). Thus, the presence of the N-terminal presequence in pro-SCP-2 resulted in less targeting to the PM caveolae/lipid rafts, consistent with the known preferential targeting of pro-SCP-2 to peroxisomes (reviewed in ref *39*).

DISCUSSION

Although a large variety of proteins that are important in cell signaling and lipid uptake/efflux reside in PM caveolae, the mechanism whereby these proteins are targeted to caveolae is not completely clear. With regard to proteins involved in signaling, to date, all are thought to directly interact with caveolin-1 through specific aa binding sequences. Each signaling protein is predicted to contain a CBD that recognizes the CSD residing in aa 80−101 of caveolin-1 (*47*). The CSD is not only important for signaling protein recognition, but also model membrane studies indicate that

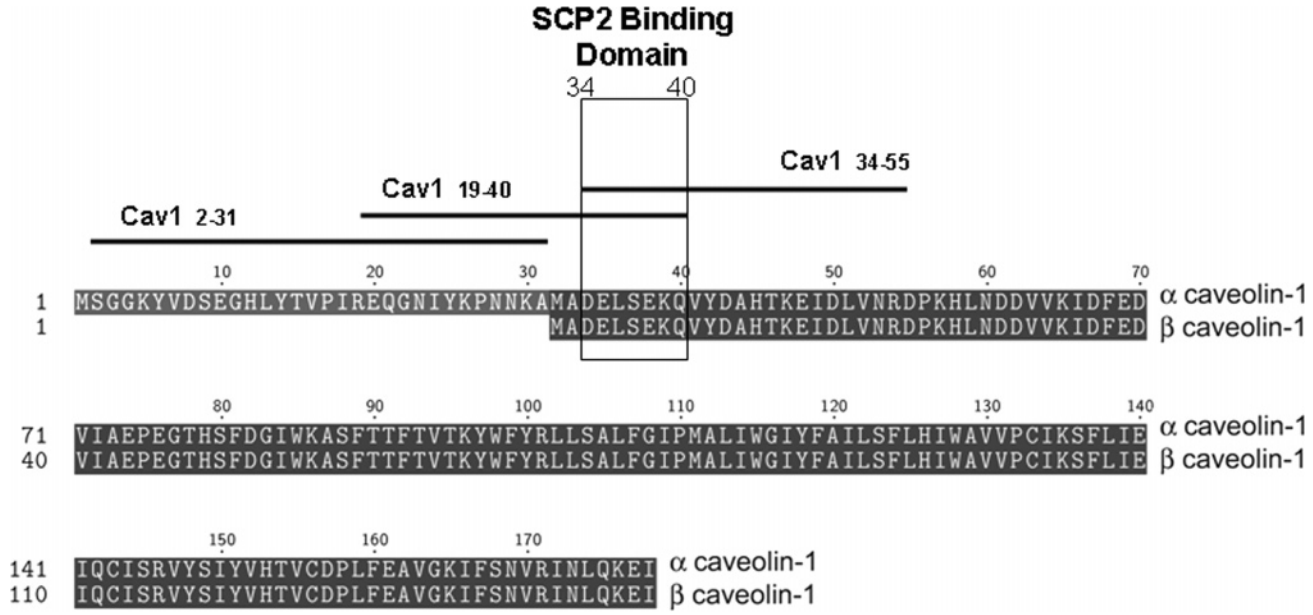

FIGURE 6: Sequence comparison of α- and *β*-caveolin-1: interaction sites with the SCP-2 N terminus. The sequences of α-caveolin-1 and *β*-caveolin-1 are aligned with three caveolin-1 peptides ($Cav1_{2-31}$, $Cav1_{19-40}$, and $Cav1_{34-55}$) to map the SCP-2 binding site. Full-length SCP-2 did not react with $Cav1_{2-31}$ but did react with both $Cav1_{19-40}$ and $Cav1_{34-55}$, which has an overlap of sequences from aa 34−40.

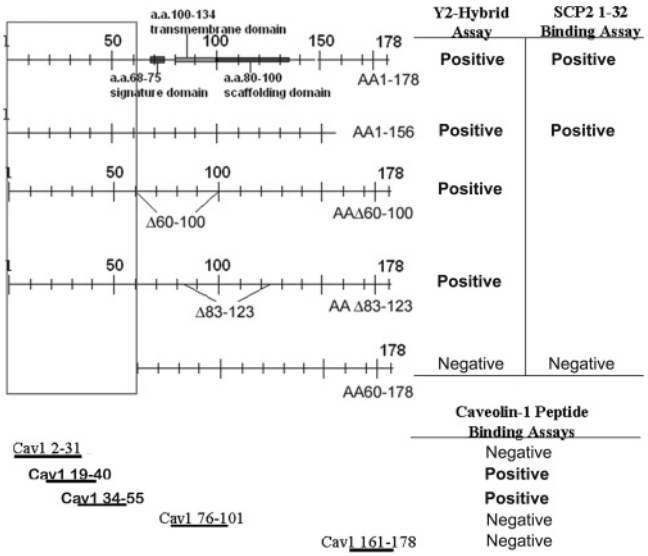

FIGURE 7: Summary of SCP-2 and caveolin-1 binding data. The known functional domains (signature domain aa 68−75, scaffolding domain aa 80−100, and transmembrane domain aa 100−134 of caveolin-1 are shown in the full-length schematic. Deletion mutations are indicated below the full-length caveolin-1. The vertical rectangle marked as residues 1−59 represents the putative binding domain of caveolin-1 to SCP-2 as defined by the results of the yeast two-hybrid assay (results on the far right). $SCP\text{-}2_{1-32}$ peptide binding assays are shown to the right of the yeast two-hybrid data. Results of the Cav1 peptide binding assays are shown at the bottom of the figure, with a linear depiction of each peptide. On the basis of these results, the SCP-2 binding domain of caveolin-1 has been delineated to residues 32−55 (horizontal rectangle). When the data are taken together, the SCP-2 binding domain for caveolin-1 mapped to SCP-2 residues 1−32 and the caveolin-1 binding domain for SCP-2 has been delineated to 23 residues.

a peptide comprised of the caveolin-1 scaffolding domain is sufficient for membrane interaction and membrane domain formation (*68*). The membrane interaction component of the scaffolding domain is mediated largely by electrostatic interactions between aa segments rich in basic aa, which interact with/recruit acidic phospholipids to form lipid rafts

Table 3: Interaction of SCP-2 and pro-SCP-2 with PEX 5C[a]

FRET pair		quenching	
donor	acceptor	K_d (nM)	R (Å)
Cy-3-PEX5C	Cy-5-SCP-2	26 ± 2	66.8 ± 0.8
Cy-3-PEX5C	Cy-5-Pro-SCP-2	2.3 ± 0.2[b]	72.4 ± 0.4[b]

[a] FRET was performed as described in the Materials and Methods to determine the binding affinity (K_d) and intermolecular distance (R). [b] $p < 0.05$ ($n = 3$) versus SCP-2.

(*68*). In contrast, because the CBD interaction motifs of signaling proteins contain very few acidic and even fewer basic aa, it is unlikely that these protein−caveolin-1 interactions occur primarily via electrostatic interactions (*48*). Instead, the CBD of interacting signaling proteins is comprised of the recognition sequence ΦXΦXXXXΦ or ΦXXXXΦXXΦ, where Φ is an aromatic aa (Trp, Phe, or Tyr) (*12*, *48*, *49*). These data suggest that the relatively hydrophobic CBD must interact with a relatively nonpolar region present within the CSD, possibly via the seven hydrophobic residues known to reside therein (*68*). An important functional feature common to almost all signaling protein/caveolin-1 interactions is that caveolin-1 association inhibits the activities of the signaling proteins while post-translational modifications (e.g., phosphorylation) disrupt such interactions and enhance the activity of signaling proteins (*47*, *48*, *68*) .

In contrast, the signaling and cholesterol homeostatic functions appear codependent (*73*). Much less is known about specific aa sequences that target proteins involved in lipid uptake/efflux to caveolae. Of the membrane-associated proteins (SRB1, ABCA1, P-gp, and caveolin-1) involved in cholesterol uptake/efflux, only two of the possible interaction pairs have been demonstrated: (i) cross-linking studies show that ABCA1 directly interacts with caveolin-1, through an as yet unresolved CBD and CSD sequences (*22*), and (ii) caveolin-1 contains the requisite CBD sequence for interacting with the caveolin CSD (*48*) and homo-oligomerizes, important for caveolae formation and function in signaling

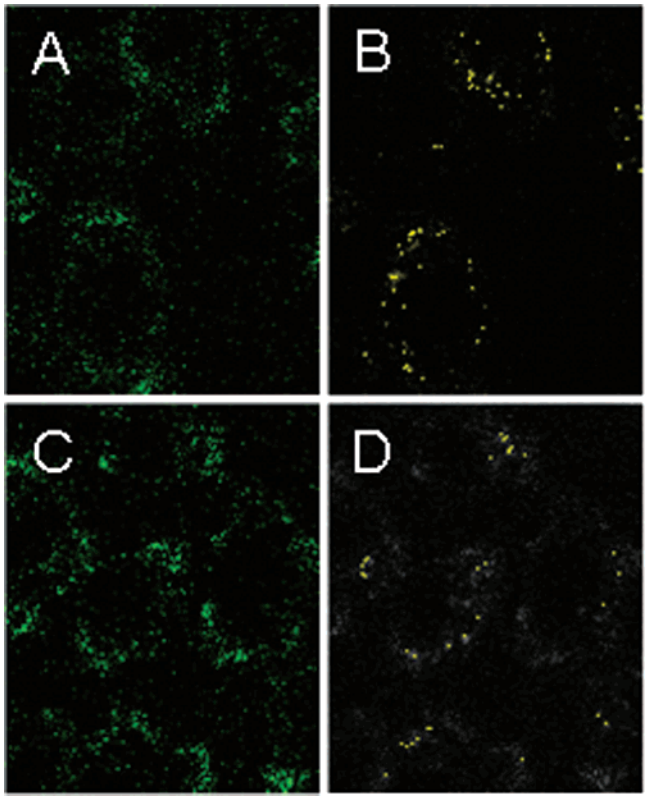

FIGURE 8: Co-localization of Cy5-SCP-2 or Cy5-proSCP-2 with cholera toxin B−Alexa Fluor 488 (AF488) in L cells. L cells were incubated with Cy5-labeled SCP-2 or Cy5-labeled proSCP-2, followed by Alexa Fluor 488-labeled cholera toxin B as described in the Materials and Methods. Laser scanning confocal microscopic images were obtained also, as described in the Materials and Methods. A, Cholera toxin B-AF488; B, Cy5-labeled SCP-2 co-localized with cholera toxin B-AF488 (yellow pixels); C, cholera toxin B-AF488; D, Cy5-labeled proSCP-2 co-localized with cholera toxin B-AF488 (yellow pixels).

and lipid transport (*11*, *34*, *48*, *68*, *74*−*76*). Of the membrane-associated proteins (SRB1, ABCA1, P-gp, and caveolin-1) involved in cholesterol uptake/efflux, only caveolin-1 has been shown to bind cholesterol *in vitro* (*17*), cross-link to photoactivatable cholesterol (*31*, *73*, *77*), and mediate bidirectional trafficking of cholesterol to and from caveolae (*17*, *25*, *78*). Phosphorylation of Ser 80 within the CSD inhibits sterol binding to caveolin-1 and stimulates cholesterol efflux from cultured cells (*73*). The fact that SCP-2 is a ubiquitous protein found in all mammalian tissues examined suggests that the SCP-2 interaction with the N terminus of caveolin-1 may facilitate cholesterol efflux when the interaction of caveolin-1 with the caveolin-1 CSD is disrupted. To date, the specific membrane protein(s) involved in cholesterol insertion into caveolae, translocation across caveolae, and desorption from caveolae remain to be identified.

Given that the scaffolding domain of caveolin-1 recognizes the binding domain of other caveolin-1 molecules, caveolin-1/caveolin-1 oligomerization may be involved in the docking of caveolar vesicles or caveolin-1/lipid/chaperone complexes that direct cholesterol and cholesteryl ester trafficking to/from caveolae (*11*, *34*, *48*, *68*, *74*, *76*). Although FRET and immunogold electron microscopy data from our laboratory suggest that SCP-2 is in sufficient proximity to caveolin-1 for direct interaction in several cultured cell lines, examination of the aa sequence indicates that this cholesterol binding/transport protein does not contain the consensus CBD necessary for interaction with the CSD (*50*). The data presented herein provided several new insights and demonstrated for the first time a potential new caveolin-1 recognition domain, independent of the CSD motif, for the interaction with proteins not containing the classic CBD domain.

Our previous data show that full-length SCP-2 and full-length caveolin-1 interact in an *in vivo* yeast two-hybrid assay. This reactivity was further shown by FRET and co-immunoprecipitation strategies, strongly suggesting a direct protein−protein interaction between these molecules (*50*). Therefore, we evaluated the interaction of caveolin-1 mutants with SCP-2 to determine if SCP-2 bound a specific caveolin-1 domain. Reactivity of purified caveolin-1 synthetic peptides and purified SCP-2 in an *in vitro* binding assay verified a direct protein−protein interaction. However, we recognize that other molecules may be involved *in vivo*. Data from the current investigation revealed the following:

First, studies with caveolin-1 mutants in the yeast two-hybrid assays demonstrated that the SCP-2 binding domain was present in the caveolin-1 N-terminal region of both α- and *β*-caveolin-1 isoforms.

Second, deletion of the α-caveolin-1 N-terminal aa 1−59 abolished binding to the SCP-2_{1-32}-bound beads. Conversely, the N-terminal α-caveolin-1 peptide (Cav_{2-31}) bound to Sepharose beads failed to bind purified SCP-2, whereas SCP-2 bound two caveolin-1 peptides, Cav_{19-40} and Cav_{34-55}, with the more N-terminal peptide showing stronger reactivity. When these result are taken together, this positive reactivity with Cav_{19-40} and Cav_{34-55} and negative reactivity with Cav_{2-31} indicated that the SCP-2 binding site encompassed caveolin-1 residues 34−50, a new caveolin-1 binding domain. It should be noted however that, because of alternate transcription sites, the caveolin-1 gene encodes for two isoforms: α-caveolin-1 and *β*-caveolin-1 (*79*, *80*). These isoforms differ in that the *β*-caveolin-1 is missing the N-terminal 32 aa (Figure 6). On the basis of the fact that the putative SCP-2 binding site for α-caveolin-1 is residues 34−40, which are also present at the N terminus of *β*-caveolin-1 (boxed area in Figure 6), it is expected that SCP-2 would interact equally well with both proteins.

Third, the C-terminal deletion mutants of α-caveolin-1 1−156 and *β*-caveolin-1 1−156 interacted with SCP-2_{1-32} and Pro-SCP-2_{1-20} by the *in vitro* peptide binding technique but only weakly bound full-length *β*-caveolin-1. These data indicate that (i) deletion of the *β*-caveolin-1 C terminus facilitates exposure of the *β*-caveolin-1 N terminus to interact with SCP-2, (ii) the α-caveolin-1 C terminus is not essential to SCP-2 binding, and (iii) the caveolin-1 C terminus influences the exposure of the caveolin-1 N terminus. This could explain earlier results in which the rotavirus protein NSP4 interacts with both termini of caveolin-1 (*54*). In this study, the N terminus of caveolin-1 was more reactive in the peptide binding assay than the C terminus of caveolin-1, perhaps because the role of NSP4 binding to the C terminus of caveolin-1 is to expose the N terminus of caveolin-1 to NSP4 for binding. Additional data are needed to verify this hypothesis, although these data are consistent with the mutant caveolin-1 SCP-2 binding results.

Fourth, deletion mutants of caveolin-1 missing all or part of the scaffolding domain (aa 80−100) interacted with SCP-2 in the yeast two-hybrid assay (CavΔ60−100 and CavΔ83−

123). These data were consistent with SCP-2 lacking the aromatic consensus CBD (*50*). Thus, SCP-2 interaction with caveolin-1 must be mediated through a domain outside of the caveolin-1 CBD. Our laboratory showed earlier that the SCP-2 N-terminal aa 1−32 has an amphipathic α-helix structure and that one face of this helix is enriched with basic residues that interact with anionic phospholipids in membranes (*52*, *63*). Because both the SCP-2 N terminus (*63*) and the CSD domain (*68*) are rich in basic aa (positively charged), this may actually result in an electrostatic repulsion between them and explain in part why SCP-2 does not bind to the CSD.

Fifth, the N-terminal aa 1−32 of SCP-2 were sufficient to provide an interaction domain for caveolin-1. The *in vitro* binding assay showed that the N-terminal peptide SCP-2_{1-32}, coupled to Sepharose beads, captured full-length α-caveolin-1 from lysates of MDCK cells or yeast expressing caveolin-1 but not yeast deficient in caveolin-1. SCP-2_{1-32}−Sepharose beads did not capture full-length β-caveolin-1 from MDCK cell lysates. Although the current findings demonstrate that N-terminal SCP-2_{1-32} interacts directly with the N-terminal binding site present in α-caveolin-1, it must be noted that the N-terminal SCP-2_{1-32} also represents the interaction domain with anionic phospholipids of model membranes (*63*, *64*). Circular dichroism (*63*, *64*), nuclear magnetic resonance (NMR), and crystallography studies show that SCP-2_{1-32} is comprised of an amphipathic α helix with hydrophobic residues facing inward into a hydrophobic tunnel (*38*, *81*, *82*). The cationic residues face outward for the interaction with membranes containing anionic phospholipids (*63*) or potentially proteins with patches of anionic residues (*38*, *81*, *82*). Caveolin-1 contains a putative α-helical domain at residues 30−40 (*78*). Modeling studies indicate that this region could interact with the α-helical region of N-terminal SCP-2 (Table 1). To disrupt the amphipathic α helix of SCP-2_{1-32}, Leu20 (L20) was replaced with Glu20 (E20). This change results in the loss of binding to anionic phospholipids (*63*, *64*) as well as the loss of both phospholipid and cholesterol transport (*70*). However, as shown herein, SCP-$2_{1-32E20}$ still interacted with full-length α-caveolin-1, suggesting that the interaction of SCP-2 with caveolin-1 was independent of its ability to bind/transfer cholesterol and phospholipid.

To date, very little is known regarding the functional significance of these two isoforms of caveolin-1 (*79*). Immunofluorescence and immunogold labeling reveal that the α- and β-caveolin-1 have distinct but overlapping distributions at the PM (*80*). On the basis of the finding that α-caveolin-1 is localized in deep caveolae, while β-caveolin-1 is localized in shallower caveolae, it has been suggested that α-caveolin-1 may have a greater potential to form caveolae (*79*). The current investigation extends the potential functional significance of these isoforms by demonstrating that only the full-length α-caveolin-1 but not the β-caveolin-1 interacted with SCP-2 and the N-terminal SCP-2_{1-32}. To our knowledge, this is the first report identifying a new protein binding site in the α-caveolin-1 isoform at the N-terminal cytoplasmic region distinct from the scaffolding domain for a cellular protein and the second report of a protein binding outside the CBD/CSD (*54*).

It is of interest to note that the 20 aa presequence present in pro-SCP-2 also interacted with the N-terminal region of caveolin-1. This N-terminal presequence is flexibly disordered in solution (*83*, *84*), suggesting that the presequence may be available for the interaction with caveolin-1. However, this interaction is not physiologically significant because (i) Western blotting detects only the mature 13 kDa SCP-2 and not the 15 kDa pro-SCP-2 in all mammalian tissues examined as well as in all transfected cells overexpressing pro-SCP-2 examined (reviewed in ref *39*); (ii) as shown in the present work, pro-SCP-2 bound nearly 12-fold better than SCP-2 to PEX5C, the receptor for the C-terminal peroxisomal targeting sequence present in both pro-SCP-2 and SCP-2. The higher affinity of PEX5C for pro-SCP-2 versus SCP-2 was recently confirmed by isothermal titration calorimetry (*83*). The enhanced affinity of the pro-SCP-2 for PEX5C is associated with greater aqueous exposure of the C-terminal peroxisomal targeting sequence 1 in pro-SCP-2 as compared to SCP-2 (*60*); (iii) the data presented herein show that, as compared to SCP-2, incorporation of pro-SCP-2 into cells resulted in less localization to GM_1, a marker for caveolae/lipid rafts at the PM. Photoactivatable GM_1 cross-links to caveolin-1 at the PM (*85*); (iv) expressing the cDNA for pro-SCP-2 in transfected cells resulted in several-fold enhanced peroxisomal targeting as compared to the expression of the cDNA encoding SCP-2 (reviewed in ref *39*); (v) in normal tissues, the highest concentration of SCP-2 is found in peroxisomes (reviewed in refs *39* and *86*); (vi) in all normal tissues and transfected cells overexpressing pro-SCP-2, the 20 aa presequence undergoes complete post-translational cleavage at the peroxisome, followed by degradation (reviewed in ref *39*); (vii) there is little difference in the localization of immunoreactive SCP-2 at the PM of cells overexpressing SCP-2 or pro-SCP-2 (*50*, *87*). Thus, the interaction of the 20 aa presequence with caveolin-1 is not likely to be of functional significance because the pro-SCP-2 protein is not detectable.

The SCP-2 interaction with the N-terminal aa 34−40 of caveolin-1 is important in cholesterol trafficking: (i) The SCP-2−N-terminal caveolin-1 interaction was highly selective for the α-caveolin-1, an isoform localized in "deep" caveolae (*79*), possibly representing more mature caveolae containing a fuller complement of proteins involved in reverse cholesterol transport (RCT); (ii) The binding site in α-caveolin-1 may provide a "docking" area for SCP-2 to influence the activity of caveolin-1 in cholesterol transport as both SCP-2 and caveolin-1 bind cholesterol. Furthermore, the N-terminal binding site of α-caveolin-1 may optimally position SCP-2 to act as either a cholesterol donor or a cholesterol acceptor to/from caveolin-1 or other proteins that interact with caveolin-1 within the caveolar membrane. For example, cross-linking studies show that caveolin-1 does not directly interact with SRB1 or HDL but instead cross-links with ABCA1, which in turn cross-links with HDL (*22*). When this finding is taken together with the data presented herein, it suggests that SCP-2 transports bound ligand (e.g., cholesterol) from intracellular sites, followed by the interaction with caveolin-1 at the PM for cholesterol efflux via ABCA1 bound to HDL or apoA1. Alternately, SCP-2 bound to α-caveolin-1 in PM caveolae may function as a cholesterol acceptor from HDL tethered to ABCA1 or SRB1 localized in caveolae. These possibilities were differentiated by studies with transfected cells overexpressing SCP-2, which support the latter possibility because these cells exhibited enhanced

cholesterol uptake (*44*), increased cholesterol transport from the PM to endoplasmic reticulum for esterification (*45*, *88*, *89*), and reduced efflux of cholesterol from lipid-storage droplets (*33*). These studies with cultured cells are further supported by findings with gene-targeted mice. In control-fed mice, SCP-2 overexpression induced hepatic cholesterol (unesterified and esterified) accumulation and potentiated the effect of a cholesterol-rich diet to further enhance hepatic cholesterol accumulation (*90*). In contrast, SCP-2/SCP-x gene ablation reduced hepatic cholesterol (especially cholesteryl ester) accumulation (*46*). When these data are taken together, they suggest that the SCP-2 interaction with caveolin-1 may facilitate cholesterol desorption from caveolae for uptake or retention into the cell rather than for efflux.

Recent reports suggest additional functional significance of the SCP-2 interaction with the N terminus of α-caveolin-1 in lipid signaling. Lipid rafts/caveolae are enriched not only in cholesterol but also in lipids involved in intracellular signaling [phosphatidylinositol (PtdIns), phosphatidylinositol-4-phosphate (PtdIns-4-P), phosphatidylinositol-4,5-bisphosphate (PtdIns-4,5-P), sphingolipids, gangliosides, ceramide, and diacylglycerol] (*47*, *51*, *78*, *91*−*93*). SCP-2 binds and enhances transfer not only of cholesterol but also PI and sphingolipids (*35*, *39*, *94*, *95*). SCP-2 overexpression redistributes PI from intracellular sites to PM caveolae/lipid rafts (*4*, *51*, *96*, *97*), redistributes select sphingolipid-signaling lipids to caveolae/lipid rafts (*97*, *98*), stimulates insulin-mediated inositol-triphosphate production (*94*), and enhances conversion of ceramide to galactosyl-ceramide (*95*). When both signaling lipids were bound and transferred, such as PI, polyphosphoinositides, and sphingolipids, the SCP-2 interaction with caveolin-1 at PM caveolae may regulate signaling within the cell (reviewed in refs *95* and *97*).

In summary, the data presented herein using the yeast two-hybrid system, an *in vitro* binding assay, and FRET demonstrated for the first time that SCP-2, specifically the N-terminal aa 1−32 amphipathic α helix, interacted with caveolin-1 at a site distinct from the C-terminal caveolin-1 scaffolding domain. Instead, SCP-2 bound caveolin-1 through a new domain identified in the α-caveolin-1 N terminus between aa 34−40. Disruption of the SCP-2 N-terminal amphipathic helical region (i.e., $SCP\text{-}2_{1-32E20}$) abolished binding to anionic phospholipids (*63*, *64*) and lipid-transfer activity (*70*) but did not inhibit SCP-2 binding to the α-caveolin-1 N terminus. This indicated that ligand binding to SCP-2 and the SCP-2 interaction with caveolin-1 were independent. While the 20 aa presequence present in pro-SCP-2 also interacts with α-caveolin-1, the physiological significance of this interaction is doubtful because (i) pro-SCP-2 is much more weakly targeted to GM_1 located in PM caveolae/lipid rafts, (ii) pro-SCP-2 has a 12-fold stronger affinity than SCP-2 for the peroxisomal receptor of the peroxisomal targeting sequence, and (iii) pro-SCP-2 is much more highly targeted than SCP-2 to peroxisomes, where the N-terminal 20 aa are cleaved such that Western blotting detects only the mature SCP-2. Finally, a more prominent interaction between SCP-2 and β-caveolin-1 was observed when the C terminus of caveolin-1 was deleted. Because α-caveolin-1 is localized primarily in deep caveolae, these findings report one of the first structurally and potentially functionally selective interactions of a soluble lipid carrier with a specific caveolin-1 isoform.

REFERENCES

1. Schroeder, F., and Nemecz, G. (1990) Transmembrane cholesterol distribution. In *Advances in Cholesterol Research* (Esfahami, M., and Swaney, J., Eds.) pp 47−87, Telford Press, Caldwell, NJ.
2. Schroeder, F., Frolov, A. A., Murphy, E. J., Atshaves, B. P., Jefferson, J. R., Pu, L., Wood, W. G., Foxworth, W. B., and Kier, A. B. (1996) Recent advances in membrane cholesterol domain dynamics and intracellular cholesterol trafficking, *Proc. Soc. Exp. Biol. Med. 213*, 150−177.
3. Schroeder, F., Gallegos, A. M., Atshaves, B. P., Storey, S. M., McIntosh, A., Petrescu, A. D., Huang, H., Starodub, O., Chao, H., Yang, H., Frolov, A., and Kier, A. B. (2001) Recent advances in membrane cholesterol microdomains: Rafts, caveolae, and intracellular cholesterol trafficking, *Exp. Biol. Med. 226*, 873−890.
4. Schroeder, F., Atshaves, B. P., Gallegos, A. M., McIntosh, A. L., Liu, J. C., Kier, A. B., Huang, H., and Ball, J. M. (2005) Lipid rafts and caveolae organization. In *Advances in Molecular and Cell Biology* (Frank, P. G., and Lisanti, M. P., Eds.) pp 3−36, Elsevier, Amsterdam, The Netherlands.
5. Schroeder, R., London, E., and Brown, D. (1994) Interactions between saturated acyl chains confer detergent resistance on lipids and glycosylphosphatidylinositol (GPI)-anchored proteins: GPI-anchored proteins in liposomes and cells show similar behavior, *Proc. Natl. Acad. Sci. U.S.A. 91*, 12130−12134.
6. Gallegos, A. M., McIntosh, A. L., Atshaves, B. P., and Schroeder, F. (2004) Structure and cholesterol domain dynamics of an enriched caveolae/raft isolate, *Biochem. J. 382*, 451−461.
7. Gallegos, A. M., Storey, S. M., Kier, A. B., Schroeder, F., and Ball, J. M. (2006) Stucture and cholesterol dynamics of caveolae/raft and nonraft plasma membrane domains, *Biochemistry 45*, 12100−12116.
8. Bretscher, M. S., and Munro, S. (1993) Cholesterol and the Golgi apparatus, *Science 261*, 1280−1281.
9. Hommelgaard, A. M., Roepstorff, K., Vilhardt, F., Torgersen, M. L., Sandvig, K., and van Deurs, B. (2005) Caveolae: Stable membrane domains with a potential for internalization, *Traffic 6*, 720−724.
10. Tagawa, A., Mezzacasca, A., Hayer, A., Longatti, A., Pelkmans, L., and Helenius, A. (2005) Assembly and trafficking of caveolar domains in the cell: Caveolae as stable, cargo triggered, vesicular transporters, *J. Cell Biol. 170*, 769−779.
11. Stralfors, P. (2005) Insulin signaling and caveolae. In *Caveolae and Lipid Rafts: Roles in Signal Transduction and Human Disease* (Lisanti, M. P., and Frank, P. G., Eds.) pp 141−169, Elsevier Academic Press, San Diego, CA.
12. Liu, P., Rudick, M., and Anderson, R. G. W. (2002) Multiple functions of caveolin-1, *J. Biol. Chem. 277*, 41295−41298.
13. Brown, M. S., and Goldstein, J. L. (1986) A receptor-mediated pathway for cholesterol homeostasis, *Science 232*, 34−47.
14. Fielding, C. J., and Fielding, P. E. (2000) Cholesterol and caveolae: Structural and functional relationships, *Biochim. Biophy. Acta 1529*, 210−222.
15. Connelly, M. A., and Williams, D. L. (2004) Scavenger receptor B1: A scavenger receptor with a mission to transport high density lipoprotein lipids, *Cur. Opin. Lipidol. 15*, 287−295.
16. Van Eck, M., Pennings, M., Hoekstra, M., Out, R., and Van Berkel, T. J. C. (2005) Scavenger receptor B1 and ATP-binding cassette transporter A1 in reverse cholesterol transport and atherosclerosis, *Cur. Opin. Lipidol. 16*, 307−315.
17. Everson, W. V., and and Smart, E. J. (2005) Caveolae and the regulation of cellular cholesterol homeostasis. In *Caveolae and Lipid Rafts: Roles in Signal Transduction and the Pathogenesis of Human Disease* (Lisanti, M. P., and Frank, P. G., Eds.) pp 37−55, Elsevier Academic Press, San Diego, CA.
18. Fielding, C. J., and Fielding, P. E. (1995) Molecular physiology of reverse cholesterol transport, *J. Lipid Res. 36*, 211−228.
19. Mendez, A. J., Lin, G., Wade, D. P., Lawn, R. M., and Oram, J. F. (2001) Membrane lipid domains distinct from cholesterol/sphingomyelin-rich rafts are involved in the ABCA1-mediated lipid secretory pathway, *J. Biol. Chem. 276*, 3158−3166.
20. Oram, J. F., and Lawn, R. M. (2001) ABCA1: The gatekeeper for eliminating excess tissue cholesterol, *J. Lipid Res. 42*, 1173−1179.
21. Yancey, P. G., Bortnick, A. E., Kellner-Weibel, G., de la Llera-Moya, M., Phillips, M. C., and Rothblat, G. H. (2003) Importance of different pathways of cellular cholesterol efflux, *Arterioscler., Thromb., Vasc. Biol. 23*, 712−719.

22. Chao, W. T., Tsai, S.-H., Lin, Y.-C., Lin, W.-W., and Yang, V. C. (2005) Cellular localization and interaction of ABCA1 and caveolin-1 in aortic endothelial cells after HDL incubation, *Biochem. Biophys. Res. Commun. 332*, 743−749.
23. Orso, E., Broccardo, C., Kaminski, W. E., Bottcher, A., Liebisch, G., Drobnik, W., Gotz, A., Chambenoit, O., Diederich, W., Langmann, T., Spruss, T., Luciani, M.-F., Rothe, G., Lackner, K. J., Chimini, G., and Schmitz, G. (2000) Transport of lipids from Golgi to plasma membrane is defective in Tangier disease patients and Abc1-deficient mice, *Nat. Genet. 24*, 192−196.
24. Wang, N., Silver, D. L., Thiele, C., and Tall, A. R. (2001) ATP-binding cassette transporter A1 (ABCA1) functions as a cholesterol efflux regulatory protein, *J. Biol. Chem. 276*, 23742−23747.
25. Fielding, C. J., and Fielding, P. E. (2001) Cellular cholesterol efflux, *Biochim. Biophys. Acta 1533*, 175−189.
26. Jodoin, J., Demeule, M., Fenart, L., Cecchelli, R., Farmer, S., Linton, K. J., Higgins, C. F., and Beliveau, R. (2003) P-glycoprotein in blood-brain barrier endothelial cells: Interaction and oligomerization with caveolins, *J. Neurochem. 87*, 1010−1023.
27. Ronaldson, P. T., Bendayan, M., Gingras, D., Piquette-Miller, M., and Bendayan, R. (2004) Cellular localization and functional expression of P-glycoprotein in rat astrocyte cultures, *J. Neurochem. 89*, 788−800.
28. Radeva, G., Perabo, J., and Sharom, F. J. (2005) P-glycoprotein is localized in intermediate density membrane microdomains distinct from classical lipid rafts and caveolar domains, *FEBS J. 272*, 4924−4937.
29. Daleke, D. L. (2007) Phospholipid flippases, *J. Biol. Chem. 282*, 821−825.
30. Cruz, J. C., Thomas, M., Wong, E., Ohgami, N., Sugii, S., Curphey, T., Chang, C. C. Y., and Chang, T.-Y. (2002) Synthesis and biochemical properties of a new photoactivatable cholesterol analog 7,7-azocholestanol and its linoleate ester in Chinese hamster ovary cell lines, *J. Lipid Res. 43*, 1341−1347.
31. Thiele, C., Hannah, M. J., Fahrenholz, F., and Huttner, W. B. (1999) Cholesterol binds to synaptophysin and is required for biogenesis of synaptic vesicles, *Nat. Cell Biol. 2*, 42−49.
32. Frolov, A., Petrescu, A., Atshaves, B. P., So, P. T. C., Gratton, E., Serrero, G., and Schroeder, F. (2000) High density lipoprotein mediated cholesterol uptake and targeting to lipid droplets in intact L-cell fibroblasts, *J. Biol. Chem. 275*, 12769−12780.
33. Atshaves, B. P., Starodub, O., McIntosh, A. L., Roths, J. B., Kier, A. B., and Schroeder, F. (2000) Sterol carrier protein-2 alters HDL-mediated cholesterol efflux, *J. Biol. Chem. 275*, 36852−36861.
34. Fielding, C. J., and Fielding, P. E. (2001) Caveolae and intracellular trafficking of cholesterol, *Adv. Drug Delivery Rev. 49*, 251−264.
35. Schroeder, F., Frolov, A., Schoer, J., Gallegos, A., Atshaves, B. P., Stolowich, N. J., Scott, A. I., and Kier, A. B. (1998) Intracellular sterol binding proteins, cholesterol transport and membrane domains. In *Intracellular Cholesterol Trafficking* (Chang, T. Y., and Freeman, D. A., Eds.) pp 213−234, Kluwer Academic Publishers, Boston, MA.
36. Fuchs, M., Hafer, A., Muench, C., Kannenberg, F., Teichmann, S., Scheibner, J., Stange, E. F., and Seedorf, U. (2001) Disruption of the sterol carrier protein 2 gene in mice impairs biliary lipid and hepatic cholesterol metabolism, *J. Biol. Chem. 276*, 48058−48065.
37. Stolowich, N. J., Frolov, A., Petrescu, A. D., Scott, A. I., Billheimer, J. T., and Schroeder, F. (1999) Holo-sterol carrier protein-2: ^{13}C-NMR investigation of cholesterol and fatty acid binding sites, *J. Biol. Chem. 274*, 35425−35433.
38. Stolowich, N. J., Petrescu, A. D., Huang, H., Martin, G., Scott, A. I., and Schroeder, F. (2002) Sterol carrier protein-2: Structure reveals function, *Cell. Mol. Life Sci. 59*, 193−212.
39. Gallegos, A. M., Atshaves, B. P., Storey, S. M., Starodub, O., Petrescu, A. D., Huang, H., McIntosh, A., Martin, G., Chao, H., Kier, A. B., and Schroeder, F. (2001) Gene structure, intracellular localization, and functional roles of sterol carrier protein-2, *Prog. Lipid Res. 40*, 498−563.
40. Fuchs, M., Lammert, F., Wang, D. Q. H., Paigen, B., Carey, M. C., and Cohen, D. E. (1998) Sterol carrier protein-2 participates in hypersecretion of biliary cholesterol during cholesterol gallstone formation in genetically gallstone susceptible mice, *Biochem. J. 336*, 33−37.
41. Hafer, A., Katzberg, N., Muench, C., Scheibner, J., Stange, E. F., Seedorf, U., and Fuchs, M. (2000) Studies with sterol carrier protein-2 (SCP-2) gene knockout mice identify liver fatty acid binding protein (FABP1) as intracellular cholesterol transporter contributing to biliary cholesterol hypersecretion and gallstone formation. *Gastroenterology 118* (4, Part 1 Supplement 2), 135.
42. Martin, G. G., Atshaves, B. P., McIntosh, A. L., Mackie, J. T., Kier, A. B., and Schroeder, F. (2005) Liver fatty acid binding protein (L-FABP) gene ablation alters liver bile acid metabolism in male mice, *Biochem. J. 391*, 549−560.
43. Martin, G. G., Atshaves, B. P., McIntosh, A. L., Mackie, J. T., Kier, A. B., and Schroeder, F. (2006) Liver fatty acid binding protein (L-FABP) gene ablation potentiates hepatic cholesterol accumulation in cholesterol-fed female mice, *Am. J. Physiol. 290*, G36−G48.
44. Moncecchi, D. M., Murphy, E. J., Prows, D. R., and Schroeder, F. (1996) Sterol carrier protein-2 expression in mouse L-cell fibroblasts alters cholesterol uptake, *Biochim. Biophys. Acta 1302*, 110−116.
45. Murphy, E. J., and Schroeder, F. (1997) Sterol carrier protein-2 mediated cholesterol esterification in transfected L-cell fibroblasts, *Biochim. Biophys. Acta 1345*, 283−292.
46. Seedorf, U., Raabe, M., Ellinghaus, P., Kannenberg, F., Fobker, M., Engel, T., Denis, S., Wouters, F., Wirtz, K. W. A., Wanders, R. J. A., Maeda, N., and Assmann, G. (1998) Defective peroxisomal catabolism of branched fatty acyl coenzyme A in mice lacking the sterol carrier protein-2/sterol carrier protein-x gene function, *Genes Dev. 12*, 1189−1201.
47. Smart, E. J., Graf, G. A., McNiven, M. A., Sessa, W. C., Engelman, J. A., Scherer, P. E., Okamoto, T., and Lisanti, M. P. (1999) Caveolins, Liquid-ordered domains, and signal transduction, *Mol. Cell. Biol. 19*, 7289−7304.
48. Couet, J., Li, S., Okamoto, M., Ikezu, T., and Lisanti, M. P. (1997) Identification of peptide and protein ligands for the caveolin-scaffolding domain, *J. Biol. Chem. 272*, 6525−6533.
49. Krajewska, W. M., and Maslowska, I. (2004) Caveolins: Structure and funciton in signal transduction, *Cell. Mol. Biol. Lett. 9*, 195−220.
50. Zhou, M., Parr, R. D., Petrescu, A. D., Payne, H. R., Atshaves, B. P., Kier, A. B., Ball, J. A., and Schroeder, F. (2004) Sterol carrier protein-2 directly interacts with caveolin-1 in vitro and in vivo, *Biochemistry 43*, 7288−7306.
51. Atshaves, B. P., Gallegos, A., McIntosh, A. L., Kier, A. B., and Schroeder, F. (2003) Sterol carrier protein-2 selectively alters lipid composition and cholesterol dynamics of caveolae/lipid raft vs non-raft domains in L-cell fibroblast plasma membranes, *Biochemistry 42*, 14583−14598.
52. Huang, H., Schroeder, F., Estes, M. K., McPherson, T., and Ball, J. M. (2004) The interactions of rotavirus NSP4 C-terminal peptides with model membranes, *Biochem. J. 380*, 723−733.
53. Parr, R. D., Storey, S. M., Mitchell, D. M., McIntosh, A. L., Zhou, M., Mir, K. D., and Ball, J. M. (2006) The rotavirus enterotoxin, NSP4, directly interacts wtih the caveolae structural protein, caveolin-1, *J. Virol. 80*, 2842−2854.
54. Huang, H., Starodub, O., McIntosh, A., Kier, A. B., and Schroeder, F. (2002) Liver fatty acid binding protein targets fatty acids to the nucleus: Real-time confocal and multiphoton fluorescence imaging in living cells, *J. Biol. Chem. 277*, 29139−29151.
55. Mir, K. D., Parr, R. D., Schroeder, F., and Ball, J. M. (2007) Rotavirus NSP4 interacts with both the amino- and carboxyl-termini of caveolin-1, *Virus Res. 126*, 105−116.
56. Gietz, R. D., and Woods, R. A. (2002) Transformation of yeast by lithium acetate/single-stranded carrier DNA/polyethylene glycol method, *Methods Enzymol. 350*, 87−96.
57. Landy, A. (1989) Dynamic, structural, and regulatory aspects of λ-site-specific recombination, *Annu. Rev. Biochem. 58*, 913−949.
58. Vidal, M. (1997) The reverse two-hybrid system. In *The Two-Hybrid System* (Bartel, P., and Fields, S., Eds.) pp 109, Oxford University Press, New York.
59. Vidal, M., Brachman, R. K., Fattaey, A., Harlow, E., and Boeke, J. D. (1996) Reverse two-hybrid and one-hybrid systems to detect dissociation of protein−protein and DNA−protein interactions, *Proc. Natl. Acad. Sci. U.S.A. 93*, 10315−10320.
60. Schroeder, F., Frolov, A., Starodub, O., Russell, W., Atshaves, B. P., Petrescu, A. D., Huang, H., Gallegos, A., McIntosh, A., Tahotna, D., Russell, D., Billheimer, J. T., Baum, C. L., and Kier, A. B. (2000) Pro-sterol carrier protein-2: Role of the N-terminal presequence in structure, function, and peroxisomal targeting, *J. Biol. Chem. 275*, 25547−25555.
61. Yamamoto, R., Kallen, C. B., Babalola, G. O., Rennert, H., Billheimer, J. T., and Strauss, J. F. I. (1991) Cloning and

expression of a cDNA encoding human sterol carrier protein 2, *Proc. Natl. Acad. Sci. U.S.A. 88*, 463−467.
62. Billheimer, J. T., Strehl, L. L., Davis, G. L., Strauss J. F., III, and Davis, L. G. (1990) Characterization of a cDNA encoding rat sterol carrier protein-2, *DNA Cell Biol. 9*, 159−165.
63. Huang, H., Ball, J. A., Billheimer, J. T., and Schroeder, F. (1999) The sterol carrier protein-2 amino terminus: A membrane interaction domain, *Biochemistry 38*, 13231−13243.
64. Huang, H., Ball, J. A., Billheimer, J. T., and Schroeder, F. (1999) Interaction of the N-terminus of sterol carrier protein-2 with membranes: Role of membrane curvature, *Biochem. J. 344*, 593−603.
65. Huang, H., Gallegos, A., Zhou, M., Ball, J. M., and Schroeder, F. (2002) Role of sterol carrier protein-2 N-terminal membrane binding domain in sterol transfer, *Biochemistry 41*, 12149−12162.
66. Hostetler, H. A., Petrescu, A. D., Kier, A. B., and Schroeder, F. (2005) Peroxisome proliferator activated receptor α (PPARα) interacts with high affinity and is conformationally responsive to endogenous ligands, *J. Biol. Chem. 280*, 18667−18682.
67. Petrescu, A. D., Payne, H. R., Boedeker, A. L., Chao, H., Hertz, R., Bar-Tana, J., Schroeder, F., and Kier, A. B. (2003) Physical and functional interaction of acyl CoA binding protein (ACBP) with hepatocyte nuclear factor-4α (HNF4α), *J. Biol. Chem. 278*, 51813−51824.
68. Wanaski, S., Ng, B. K., and Glaser, M. (2003) Caveolin scaffolding region and the membrane binding region of Src form lateral membrane domains, *Biochemistry 42*, 42−46.
69. Ikonen, E., Heino, S., and Lusa, S. (2004) Caveolins and membrane cholesterol, *Biochem. Soc. Trans. 32*, 121−123.
70. Seedorf, U., Scheek, S., Engel, T., Steif, C., Hinz, H. J., and Assmann, G. (1994) Structure−activity studies of human sterol carrier protein 2, *J. Biol. Chem. 269*, 2613−2618.
71. Schroeder, F., and Kier, A. B. (1983) Lipid composition alters phagocytosis of fluorescent latex beads, *J. Immunol. Methods 57*, 363−371.
72. Schroeder, F., and Kinden, D. A. (1983) Measurement of phagocytosis using fluorescent latex beads, *J. Biochem. Biophys. Methods 8*, 15−27.
73. Fielding, P. E., Chau, P., Liu, D., Spencer, T. A., and Fielding, C. J. (2004) Mechanism of platelet derived growth factor dependent caveolin-1 phosphorylation: Relationship to sterol binding and the role of serine-80, *Biochemistry 43*, 2578−2586.
74. Feron, O. (2005) The caveolin interaction with endothelial nitric oxide synthase (eNOS). In *Caveolae and Lipid Rafts: Roles in Signal Transduction and the Pathogenesis of Human Disease* (Lisanti, M. P., and Frank, P. G., Eds.) pp 91−108, Elsevier Academic Press, San Diego, CA.
75. Monier, S., Dietzen, D. J., Hastings, W. R., Lublin, D. M., and Kurzchalia, T. V. (1996) Oligomerization of VIP21-caveolin in vitro is stabilized by long chain fatty acylation or cholesterol, *FEBS Lett. 388*, 143−149.
76. Igarashi, K., Kaneda, M., Yamaji, A., Saido, T. C., Kikkawa, U., Ono, Y., Inoue, K., and Umeda, M. (1995) A novel phosphatidylserine-binding peptide motif defined by an anti-idiotypic monoclonal antibody. Localization of phosphatidylserine-specific binding sites on protein kinase C and phosphatidylserine decarboxylase, *J. Biol. Chem. 270*, 29075−29078.
77. Fielding, P. E., Russell, J. S., Spencer, T. A., Hakamata, H., Nagao, K., and Fielding, C. J. (2002) Sterol efflux to apolipprotein A-1 originates from caveolin-rich microdomains and potentiates PDGF-dependent protein kinase activity, *Biochemistry 41*, 4929−4937.
78. Smart, E. J., and van der Westhuyzen, D. R. (1998) Scavenger receptors, caveolae, caveolin, and cholesterol trafficking. In *Intracellular Cholesterol Trafficking* (Chang, T. Y., and Freeman, D. A., Eds.) pp 253−272, Kluwer Academic Publishers, Boston, MA.
79. Fujimoto, T., Kogo, H., Nomura, R., and Une, T. (2001) Isoforms of caveolin-1 and caveolar structure, *J. Cell Sci. 113*, 3509−3517.
80. Scherer, P. E., Tan, Z., Chun, M., Sargiacomo, M., Lodish, H. F., and Lisanti, M. P. (1995) Caveolin isoforms differ in their N-terminal protein sequence and subcellular distribution, *J. Biol. Chem 270*, 16395−16401.
81. Garcia, F. L., Szyperski, T., Dyer, J. H., Choinowski, T., Seedorf, U., Hauser, H., and Wuthrich, K. (2000) NMR structure of the sterol carrier protein-2: Implications for the biological role, *J. Mol. Biol. 295*, 595−603.
82. Choinowski, T., Hauser, H., and Piotnek, K. (2000) Structure of sterol carrier protein 2 at 1.8 Å resolution reveals a hydrophobic tunnel suitable for lipid binding, *Biochemistry 39*, 1897−1902.
83. Stanley, W. A., Filipp, F. V., Kursula, P., Schuller, N., Erdmann, R., Schliebs, W., Sattler, M., and Wilmanns, M. (2006) Recognition of a functional peroxisome type 1 target by dynamic import receptor Pex5p, *Mol. Cell 24*, 653−663.
84. Weber, F. E., Dyer, J. H., Garcia, F. L., Werder, M., Szyperski, T., Wuthrich, K., and Hauser, H. (1998) In pre-sterol carrier protein 2 (SCP2) in solution the leader peptide is flexibly disordered, and residues 21−143 adopt the same globular fold as in mature SCP-2, *Cell. Mol. Life Sci. 54*, 751−759.
85. Pitto, M., Brunner, J., Ferraretto, A., Ravasi, D., Palestini, P., and Masserini, M. (2000) Use of a photoactivatable GM1 ganglioside analogue to assess lipid distribution in caveolae bilayer, *Glycoconjugate J. 17*, 215−222.
86. Keller, G. A., Scallen, T. J., Clarke, D., Maher, P. A., Krisans, S. K., and Singer, S. J. (1989) Subcellular localization of sterol carrier protein-2 in rat hepatocytes: Its primary localization to peroxisomes, *J. Cell Biol. 108*, 1353−1361.
87. Starodub, O., Jolly, C. A., Atshaves, B. P., Roths, J. B., Murphy, E. J., Kier, A. B., and Schroeder, F. (2000) Sterol carrier protein-2 immunolocalization in endoplasmic reticulum and stimulation of phospholipid formation, *Am. J. Physiol. 279*, C1259−C1269.
88. Frolov, A., Woodford, J. K., Murphy, E. J., Billheimer, J. T., and Schroeder, F. (1996) Spontaneous and protein-mediated sterol transfer between intracellular membranes, *J. Biol. Chem. 271*, 16075−16083.
89. Frolov, A. A., Woodford, J. K., Murphy, E. J., Billheimer, J. T., and Schroeder, F. (1996) Fibroblast membrane sterol kinetic domains: Modulation by sterol carrier protein 2 and liver fatty acid binding protein, *J. Lipid Res. 37*, 1862−1874.
90. Atshaves, B. P., McIntosh, A. L., Landrock, D., Payne, H. R., Schroeder, F., and Kier, A. B. (2007) Sterol carrier protein-2 expression in female transgenic mice potentiates diet-induced hepatic cholesterol accumulation, *Lipids*, manuscript submitted.
91. Anderson, R. G. W. (1993) Plasmalemmal caveolae and GPI-anchored membrane proteins, *Cell Biol. 5*, 647−652.
92. Anderson, R. (1998) The caveolae membrane system, *Ann. Rev. Biochem. 67*, 199−225.
93. Waugh, M. G., Lawson, D., Tan, S. K., and Hsuan, J. J. (1998) Phosphatidyl 4-phosphate synthesis in immunoisolated caveolae-like vesicles and low buoyant non-caveolar membranes, *J. Biol. Chem. 273*, 17115−17121.
94. Schroeder, F., Zhou, M., Swaggerty, C. L., Atshaves, B. P., Petrescu, A. D., Storey, S., Martin, G. G., Huang, H., Helmkamp, G. M., and Ball, J. M. (2003) Sterol carrier protein-2 functions in phosphatidylinositol transfer and signaling, *Biochemistry 42*, 3189−3202.
95. Milis, D. G., Moore, M. K., Atshaves, B. P., Schroeder, F., and Jefferson, J. R. (2006) Sterol carrier protein-2 expression alters sphingolipid metabolism in transfected mouse L-cell fibroblasts, *Mol. Cell. Biochem. 283*, 57−66.
96. Incerpi, S., Jefferson, J. R., Wood, W. G., Ball, W. J., and Schroeder, F. (1992) Na pump and plasma membrane structure in L-cell fibroblasts expressing rat liver fatty acid binding protein, *Arch. Biochem. Biophys. 298*, 35−42.
97. Schroeder, F., Atshaves, B. P., McIntosh, A. L., Gallegos, A. M., Storey, S. M., Parr, R. D., Jefferson, J. R., Ball, J. M., and Kier, A. B. (2007) Sterol carrier protein-2: New roles in regulating lipid rafts and signaling, *Biochim. Biophys. Acta*, in press.
98. Atshaves, B. P., Jefferson, J. R., Kier, A. B., and Schroeder, F. (2007) Sterol carrier protein-2, a new sphingolipid binding protein, alters sphingolipid distribution in plasma membrane caveolae/lipid raft domains, *Biochem. J.*, manuscript submitted.

BI7002636